E-Circuit Motors & Massachusetts Maritime Academy

Motor Project Final Report

Date: 6/14/2019

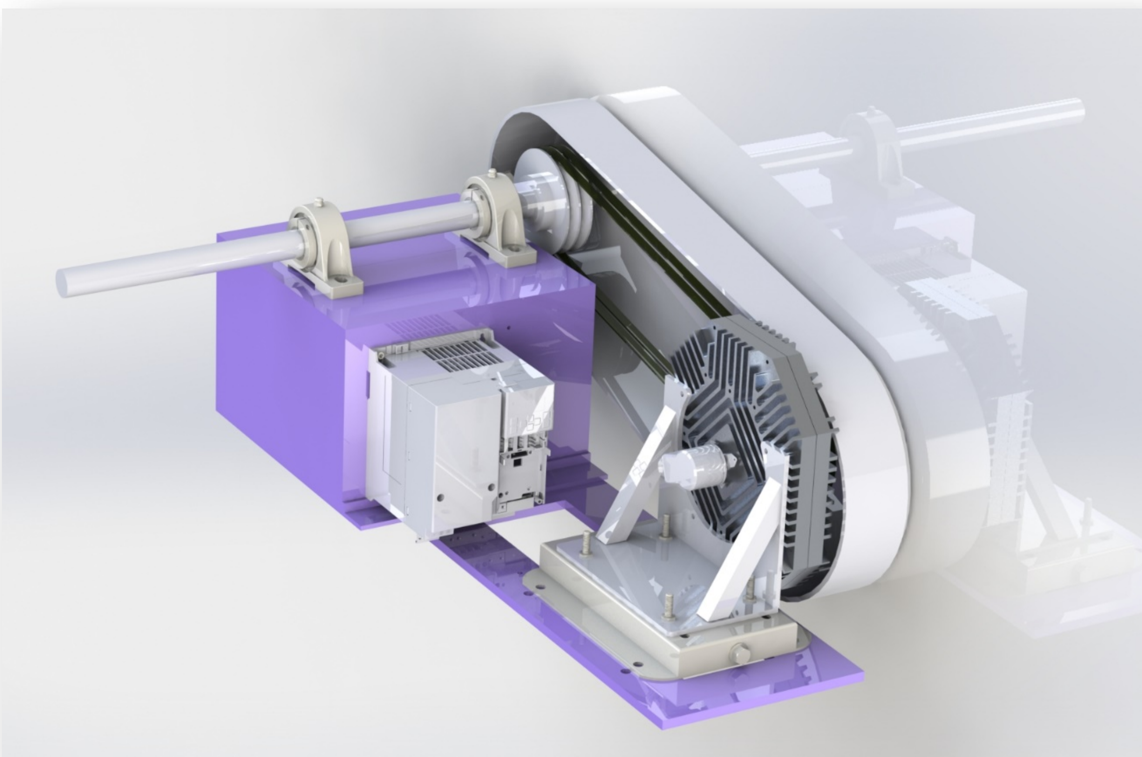

Abstract

E-Circuit Motors (ECM) in collaboration with The Massachusetts Maritime Academy (MMA) developed a detailed specification that documents the existing motor and system performance characteristics and identifies potential areas of improvement for a 3hp air handler motor on board the MMA training ship, the TS Kennedy. ECM can provide significant advantages in both cost and performance if the application is viewed as a complete system. In addition to cost sharing the project with MARAD, it is MMA's intent to utilize the oversight of The American Bureau of Shipping (ABS), MMA faculty, and cadets.

The motor ECM designed and installed was a remarkable machine that was able to cut the motor envelope and weight by almost two thirds. Both the ECM team and MMA learned a great deal with regards to shipboard power and how an application like this can greatly benefit certain areas within the maritime industry. Although the efficiency numbers were not what ECM was hoping for, better controllers and additional modifications to the motor assembly would help reach the modelled performance.

The following report outlines both the data recorded from the shipboard tests and laboratory tests as well as includes an analysis on why the results may have been the way they were. It is ECM's hope that a second iteration would be developed to improve upon the lessons learned and provide an even better solution than the one already developed.

Executive Summary

Project Summary

The goal for the project was to demonstrate ECM technology in a field application aboard the TS Kennedy as part of a MARAD-funded META demonstration project. The design, installation and testing was completed between September 2018 and April 2019. The demonstration project consisted of the replacement of an existing 3 HP motor with a motor from ECM. This motor was driving a ventilation fan by way of a pulley system on the ship.

Findings

Motor efficiency

The prototype motor generally matched (within 1.5%) of the nameplate efficiency of the existing induction motor of 89%. Further technical evaluation shows areas that need to be improved in the design and construction of the ECM motor to achieve the theoretical efficiency of 91.5% (see Appendix A). It was also noted that this project was a direct replacement of a pulley fan system and there is a potential to improve the overall system efficiency by installing the ECM motor as a direct drive motor. This would improve the overall efficiency of the system using the ECM motor.

Motor weight

The most significant advantage to the installation of ECM technology was the weight advantage as the replacement motor weighed approximately 70% lighter than the original induction machine. This is significant, as ECM's weight savings potential could be applied across all similar motors on a vessel. These weights savings would ultimately allow a vessel to carry more fuel or cargo for its particular voyage, or simply reduce the ships draft to lower drag during regular operation. On smaller vessels such as fast ferries, the weight reduction may also reduce horsepower requirements. The magnitude of weights savings will be proportional to the number of motors on the vessel.

A paper written by Hinrich Helms and Udo Lambrecht goes into more detail on the potential energy savings from reducing weight in a variety of transportation specific vehicles with high-speed ferries being one of the vessels of interest. (see appendix C)

Executive Summary Conclusion

Overall this was a successful demonstration project in that the ECM motor performed the intended function. The motor design, installation and performance were reviewed by ABS (American Bureau of Shipping) and a statement of maturity was issued (see Appendix B). Although the efficiency of the motor did not reach the theoretical efficiency, it generally matched the existing motor efficiency. We were able to identify a few key areas that can be improved in the design and construction of the ECM motor to approach the theoretical performance. Finally, the motor weight savings of 70% per motor offers the opportunity to reduce the overall ship weight substantially.

Table of Contents

Abbreviations

ABB	Asea Brown Boveri
ABS	American Bureau of Shipping
CFD	Computational Fluid Dynamics
DUT	Device Under Test
ECM	E-Circuit Motors
FOD	Foreign Objects & Debris
kg	Kilo Gram
k-Gauss	Kilo Gauss
kW	Kilo Watt
LCR	Inductance Capacitance Resistance
MARAD	U.S. Maritime Administration
META	Maritime Environmental and Technical Assistance Program
MMA	Massachusetts Maritime Academy
N-m/A	Newton Meter per Ampere
N-m	Newton Meters
PCB	Printed Circuit Board
RPM	Revolutions per minute
VFD	Variable Frequency Drive
W-Hr	Watt Hours

Initial Motor Comparisons

DATE FEBRUARY 23, 2007	OUTLINE DIMENSIONS	MOTOR TYPE: ASHH
CATALOG NO. DHP0034	3-PHASE INDUCTION MOTOR	FRAME NO. 182T

Pole	HP	KW	Hz	VOLT	Syn. Speed RPM
4	3	2.2	60	230/460	1800

Ins	Rating	Dimension in	Approx Weight	Bearings
F	CONT.	inch	95 lbs.	DE: 6306ZZ NDE: 6306ZZ

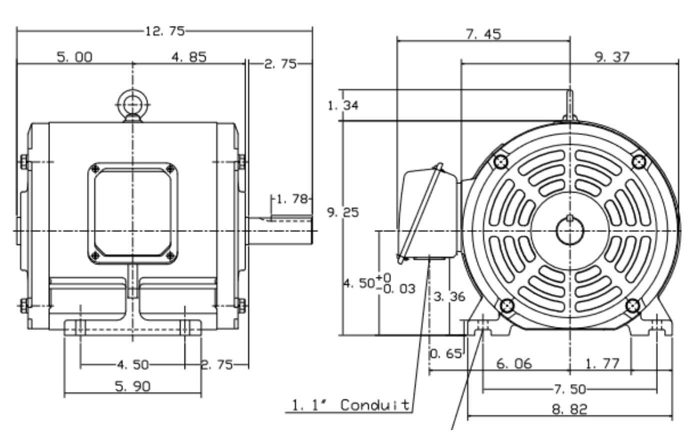

TYPICAL PERFORMANCE

FULL LOAD RPM	EFFICIENCY FULL LOAD MIN. %	EFFICIENCY FULL LOAD NOM. %	EFFICIENCY 3/4 LOAD %	EFFICIENCY 1/2 LOAD %	POWER FACTOR F. L. %	POWER FACTOR 3/4 LOAD %	POWER FACTOR 1/2 LOAD %	MAXIMUM POWER FACTOR CORRECTION
1755	87.5	89.5	89.5	87.5	81	75	62.5	1.6 KVAR

E-Circuit Motors – MMA24

3 Phase Axial Flux Permanent Magnet Motor

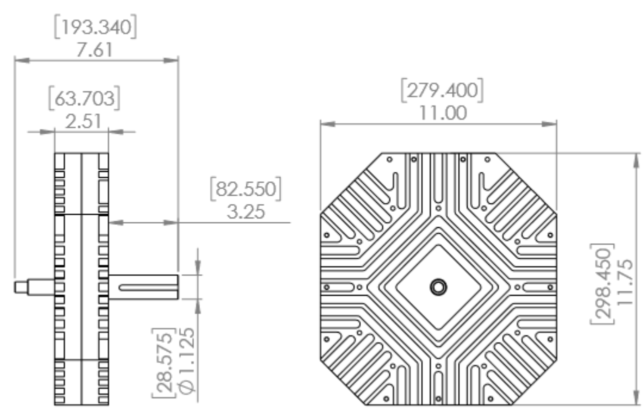

Modelled Motor Performance						
RPM	Torque [N-m]	kW In	kW Out	Efficiency	Volts	Weight [kg]
1760	11.95	2.4	2.2	91.6	48.0	12.57

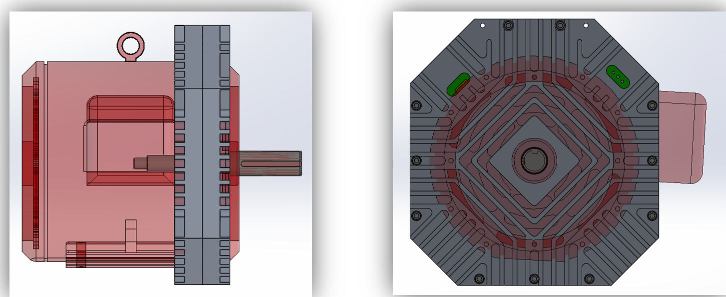

Figure 01: Induction Motor and ECM Motor Overlay Screenshots

The initial motor comparison identifies several areas of potential improvement the ECM motor could provide with the most obvious being the build envelope and weight. Even when adding the additional weight of the 90° motor frame (8.22lbs approx.), ABB controller (6.6lbs approx.), and the inductors and encoder (2.0lbs approx.), the total weight of the ECM system (44lbs approx.) was less than half the weight of the original induction motor. The other attractive benefit of the ECM motor was the potential efficiency gain, albeit only 2%. This claim would be put to the test however, since the modelled efficiency is not for the entire system (motor + controller) but instead just the motor efficiency.

Motor Installation

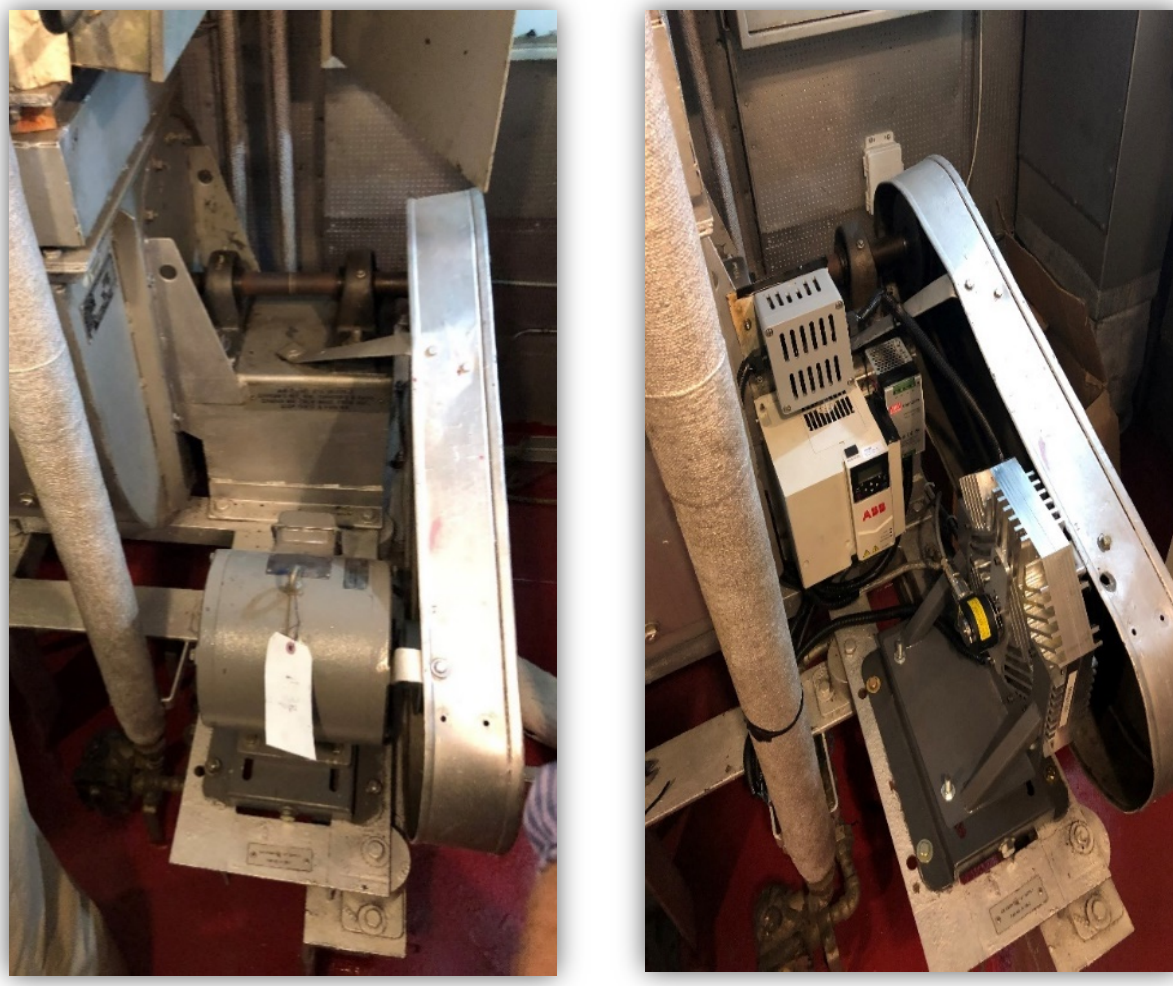

Figure 02: ECM Motor Installation Before and After

During the installation, the motor was integrated into the existing belt/pulley system with minimal changes to the previous set-up. Some of these changes included drilling additional mounting holes for the controller and inductor box as well as adjusting the pulley alignment. After seeing the install before and after, the space savings of the ECM motor becomes apparent.

Although the scope of the work required ECM to provide a “drop in” replacement to the pre-existing induction motor, the better solution would have been to integrate the ECM motor as a direct drive with the motor housing being flush against the side of the fan shroud. This would allow the removal of the belts, pulleys, and frames to further reduce the overall system weight, minimize the number of parts, and increase overall system efficiency.

Shipboard Results and Discussion

For the shipboard data collection, a HOBO H21 smart data logger was used to record several variables relating to both the ambient conditions as well as installed motor temperature and performance. The raw data retrieved from the data logger can be seen plotted below in figure 03. There are four temperature measurements in blue, a relative humidity measurement in green as well as a "pulse count" recorded by the watt node in black. This watt node is of the 20amp, 480V, 3 Phase Delta (3D - 480) variety which has a pulse scaling factor of 1.1542 WHr/pulse as listed on page 25, table 6 of the WattNode® Pulse Installation and Operation Manual. (Continental Control Systems LLC, 2011)

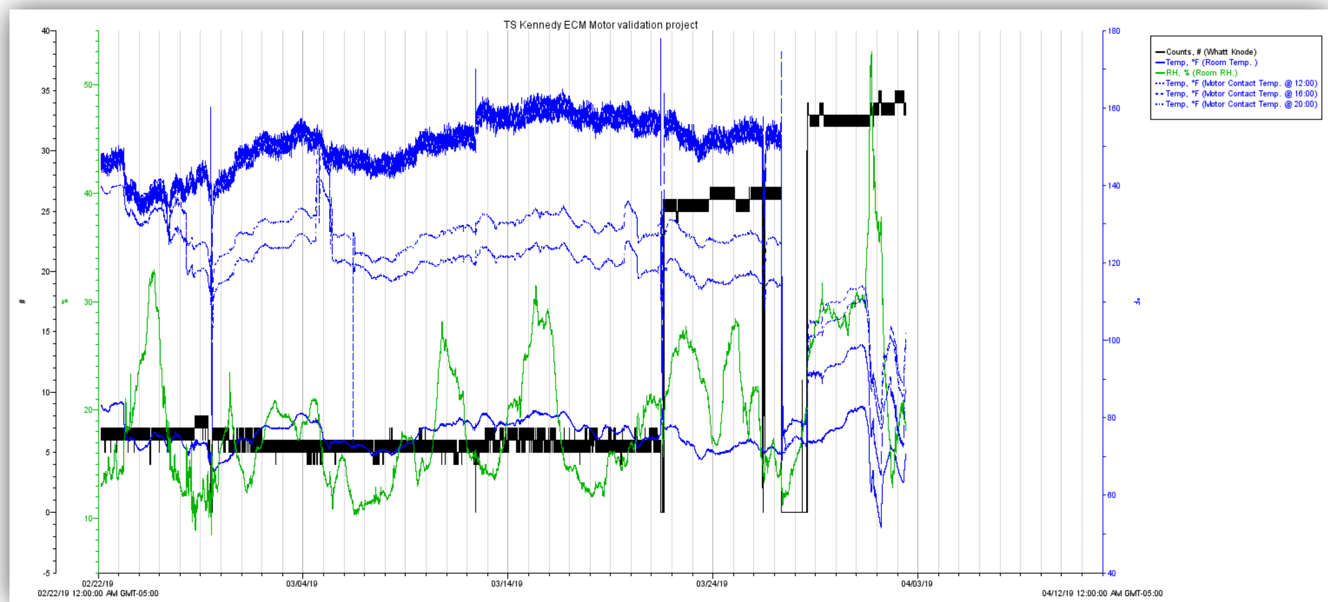

Figure 03: Data Logger Recorded Values from 2/22/2019 to 4/2/2019

The data logger recorded measurements every minute, including the number of pulses. Due to an unforeseen glitch in the Watt Node installation, the pulse calculations before 3/21/2019 were deemed unusable and were ignored in the analysis. After fixing the Watt Node and confirming the measurements were correct, the power use of each installed motor was calculated which formed the basis of the shipboard motor performance analysis.

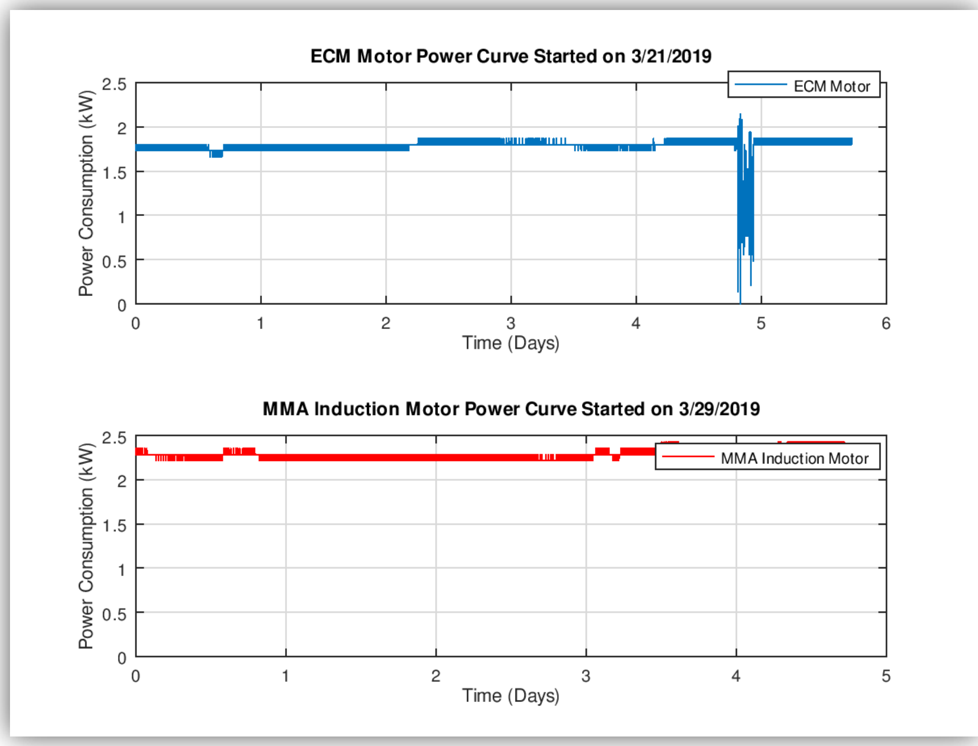

Figure 04: ECM Motor vs. MMA Induction Motor Power Use During Operation Period

Figure 04 above illustrates the relatively constant power use of each motor over the course of a couple days. It is important to note that these motors were not running at the same time, and instead had to be swapped out at the conclusion of one motor's test period. It appears the ECM motor was shut off for a couple hours before it completed its fifth day of operation.

Initial observations would indicate a considerable efficiency increase by the ECM motor due to its lower power use. However, this is not the case as further inspection revealed the ECM motor was not running at the same operating point as the original induction motor. Confusion in the incorrect watt node readings provided the ECM team with false operating point conditions which ultimately led to the selection of an inadequate motor controller to provide the required power.

ECM would have liked to replace the controller with one that was adequate for all the performance tests, however there were limitations to being able to accomplish this. The project concept was to purchase an existing, off the shelf, compatible controller within the project timeline and with the allocated funds in that area of the project scope. Due to the incorrect watt node readings, ECM ended up selecting their controller off a false operating point. During the bench tests, the motor was able to easily achieve the false operating point condition with the selected controller. However, upon realizing the operating point was different, order lead times for larger controllers would be too long to receive it in time to perform the shipboard tests within the project timeline.

Although the controller was not able to meet the power demand of the actual operating point, subsequent testing with an adequate motor controller would be possible. This would of course require additional funding and a new project plan with a clear indication on what the desired outcome should be.

Even with the inadequate motor controller limiting the conclusions that could be made from the project, further analysis was conducted to get a better understanding of the potential motor performance if this wasn't the case.

In order to gather more information on the ECM motor performance in the shipboard installation, a series of trials were conducted at different RPM settings to see how the power use changed. This was possible for the ECM motor due to the VFD controller. The same tests could not be conducted on the MMA induction motor as that is set up for constant speed and it was outside the project scope to perform a similar test on that machine. The motor speed was changed every 20 minutes in an attempt to reach both power and thermal equilibrium. Figure 05 below shows a good illustration of the changes in power at each RPM setting with power equilibrium being achieved within seconds as expected.

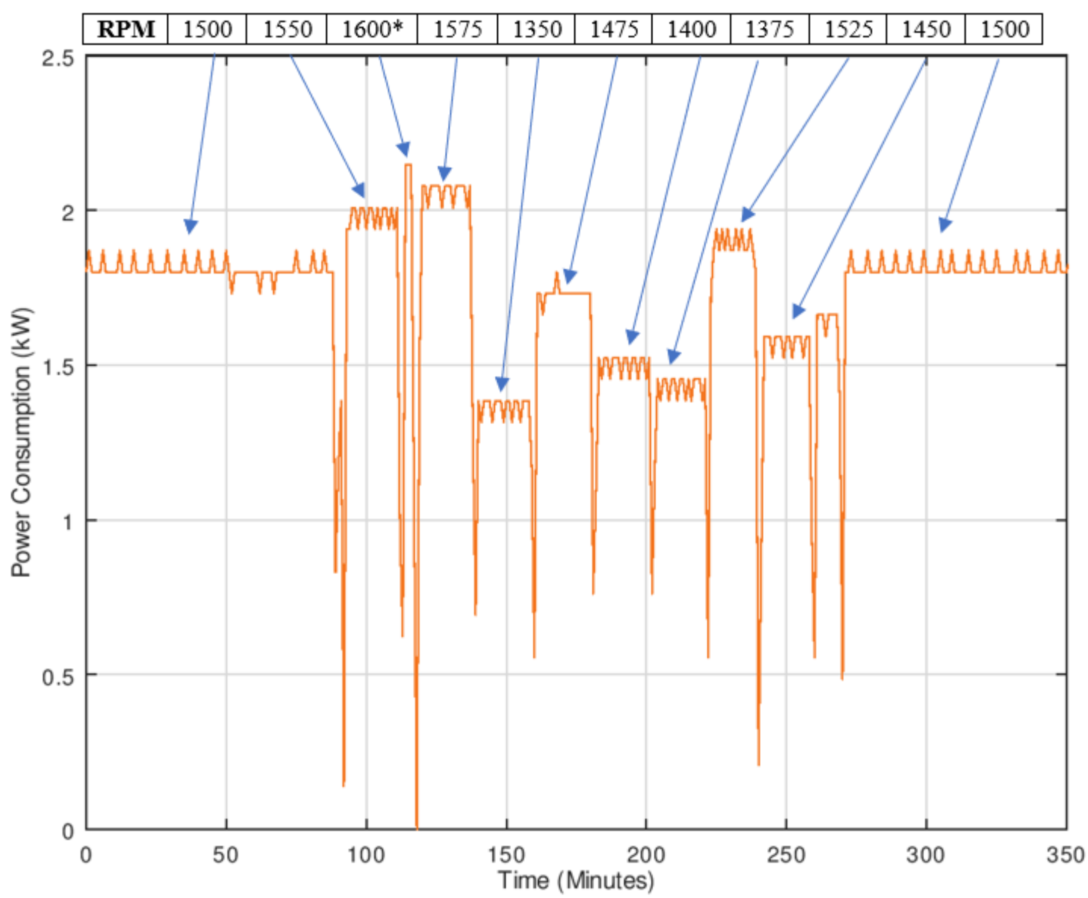

Figure 05: ECM Motor Power Use at Different RPM Ranges

After determining the RPM setting, the average power at each setting was recorded in table 01. Each RPM trial "start/stop" point was excluded from the calculation to eliminate end point outliers.

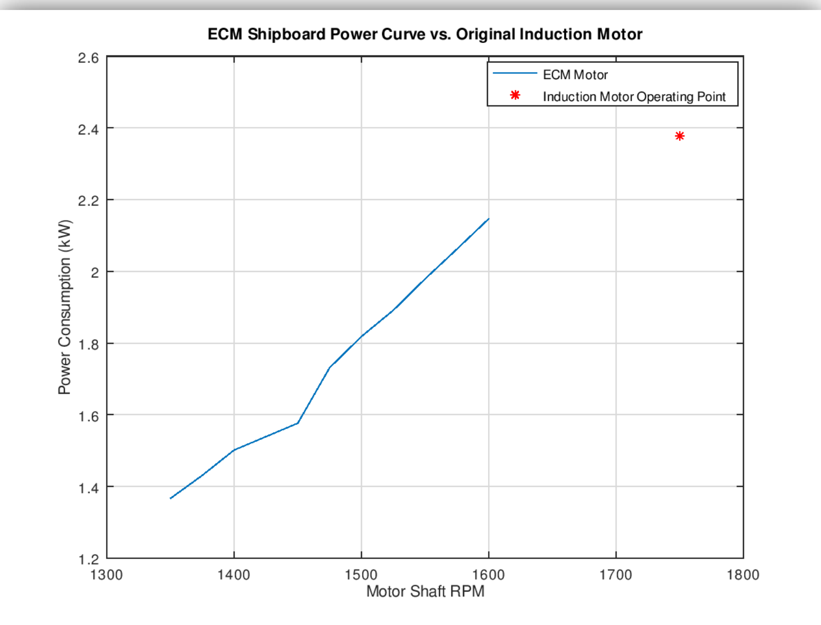

Motor Shaft RPM	Average Power Consumption (kW)
1350	1.367
1375	1.431
1400	1.502
1450	1.577
1475	1.731
1500	1.818
1525	1.891
1550	1.979
1575	2.062
1600	2.147

Figure 06 & Table 01: ECM Motor Shipboard Average kW Use @ Range of RPM vs. Original Induction Motor Operating Point

Due to the initial Watt Node measurement glitch and utilizing a new motor controller in the installation, ECM was limited to a 1600RPM shaft speed. This shaft speed was confirmed via the shaft mounted encoder. In order to check whether this was the correct speed or not for a direct comparison, the data sheet for the induction machine was referred to along with a direct measurement with a digital tachometer. The data sheet of the DHP0034 induction machine listed a synchronous speed of 1800RPM and an actual shaft speed of 1755RPM. The pulley ratio was 1:1.167 and the tachometer measured "fan shaft speed" with the induction motor was 2050RPM, yielding an actual shaft speed of 1757RPM, essentially exactly what the datasheet listed.

Clearly, the ECM motor was running over 150RPM less than the desired operating point. The motor controller would reach its current limit and fault out if a higher RPM was requested. This ultimately limited the upper power band even though that was what the ECM motor was designed to reach. This made a direct comparison impossible.

A crude interpolation up to the 1755RPM operating point would yield a power consumption of 2.66kW for the ECM motor. This would indicate a *higher* power consumption than the induction machine however this involves several assumptions. Since the motor was designed for that exact operating point, in theory the efficiency would be at its highest and thus the power consumption would not follow a linear trend as the speed is increased up to this point. Perhaps more convincing results would be possible but for the time being, these assumptions on theoretical motor performance will not be considered.

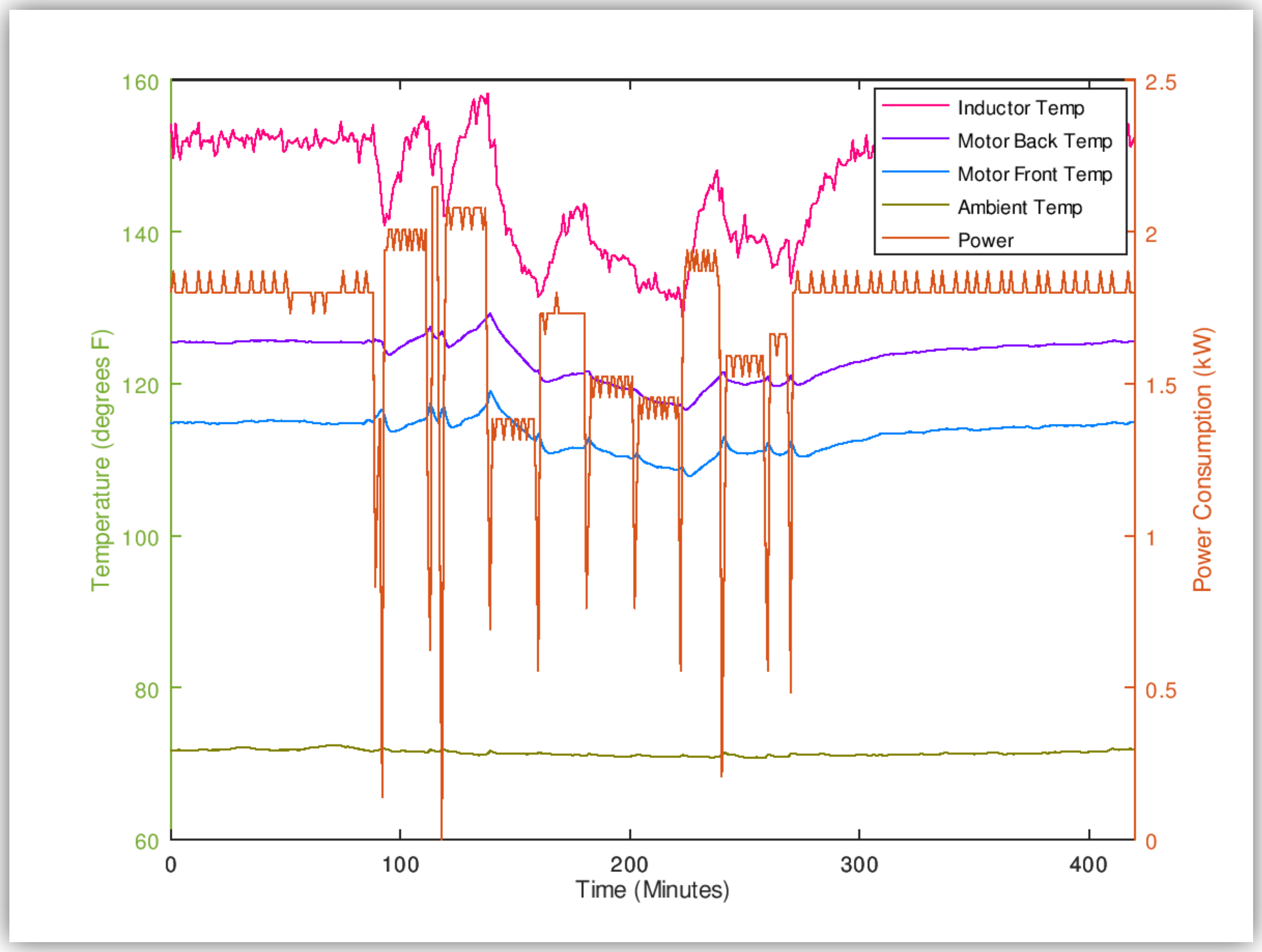

Figure 07: ECM Motor Power Use with Temperature Readings from Motor and Inductors

The purpose of the graph in Figure 07 is to show if the motor/inductors reached thermal equilibrium after each RPM change during the "RPM Time Trials". Although the peak temperature conditions occurred at the end of each *increasing* RPM test, a closer inspection of the actual temperature fluctuations indicate swings of only five degrees or so with small gradients towards the end of each RPM test. This would indicate thermal equilibrium was within a couple minutes of being reached.

The inductors are rated up to 230°F while the motor case exterior should not exceed 170°F. It is important to note the motor was relying upon free convection to cool itself during the shipboard test. The front of the motor is almost 10°F cooler than the back side of the motor due to the belts providing some air circulation on that side. Although it is designed to cool itself via free convection at the 1755RPM operating point, a fan would virtually eliminate any potential risk of the motor overheating and would ideally be implemented if a higher current capable motor controller was used. Additionally, a more efficient controller would limit the losses going to the motor and further reduce the temperature rise witnessed in the shipboard (and bench) tests.

Laboratory Testing and Discussion

During the laboratory testing, several tests were completed to help characterize the motor and identify how accurate the motor model was to the actual motor performance. Several of these tests include determining system, controller and motor efficiency, verifying the motor constants, gauss measurements to check for flux leakage, thermal tests and measuring additional windage/bearing losses.

As previously identified in the shipboard results, the controller selected for this project was undersized for what the motor requirements were supposed to be at the operating point. Regardless, power consumption data for the *system* was captured over the controller operating range (see figure 08 below). These numbers were overlaid against the values recorded from the shipboard tests. If the numbers were substantially different, that would indicate two things. Either one of the controllers was performing inadequately, or the supply power was slightly different.

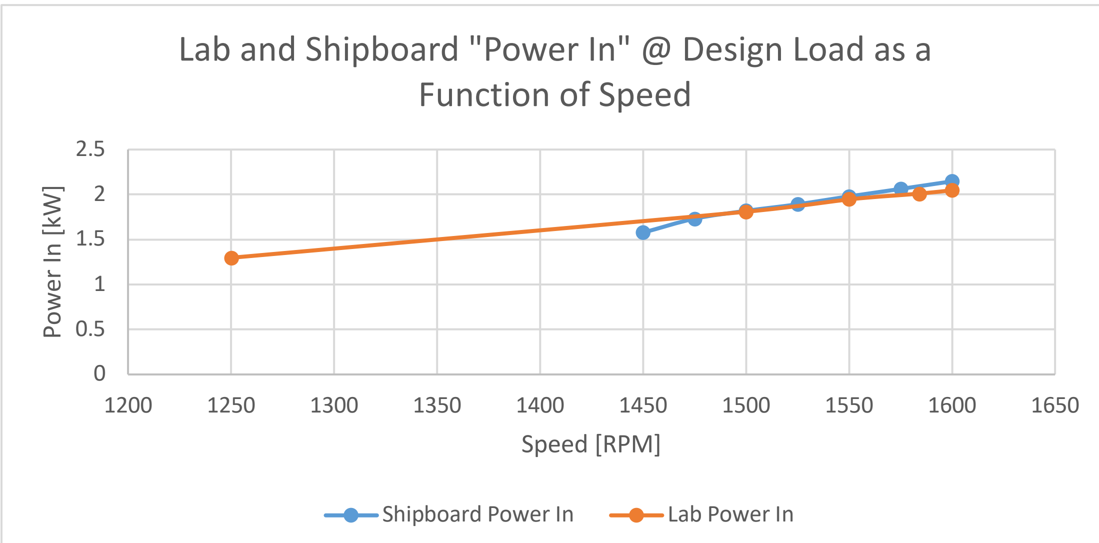

Figure 08: Lab and Shipboard Power Consumption Comparison

As expected, almost identical values were recorded between the two motor set-ups with the laboratory values slightly less than the levels on the ship which could be due to several reasons. The power source was different for both tests, and upon measuring the power going into the motor controller on the ship, a slight imbalance across the three phases was observed which could have led to some additional losses. Additionally, the motor tests in the lab setting were more controlled, especially with regards to the physical set-up without the belts and pulleys, lower ambient temperatures and optimized controller and inductor placement for cooling. Vibrations were also kept to a minimum with a rigid test stand as opposed to the MMA installation in which the motor was cantilevered off the side of the fan assembly.

Verifying the motor constants is important not only from a customer's perspective, but for the development of the ECM motor model since the recorded values are fed back in to help perfect the expected performance for future designs. The voltage constant and torque constant were verified using both current and torque readings in conjunction with a spin down test. While the motor was running at the max condition the controller would allow, the current being feed into the motor as well as the torque produced was used to calculate the motor torque constant. The average value recorded in the back to back test was 0.373 N-m/A which has a 1.1% difference than the predicted value of 0.369. The average voltage constant from the spin down test was 0.428 V-s/rad which is a percent difference of less than 0.3% of the predicted value of 0.427.

Motor efficiency was an additional benefit ECM wanted to improve upon for this project. The initial motor modelling predicted an efficiency of 91.6%. The actual system efficiency is hard to predict upfront unless the controller and power source are known at the time of motor modelling. ECM performed two sets of efficiency tests where the motor was driven via the ABB controller as well as it being run as a generator with a 3hp Baldor motor driving it. The first set up with the ABB controller provided a max efficiency of 82.84%. The second test with the ECM motor being run as a generator provided a max efficiency of 87.22%. The generator test configuration eliminates losses due to ripple and switching effects that reduce efficiency when a drive is used. Motor use requires a drive, but these losses can be minimized by optimization of the drive and filter. Also, note that generator testing allows an approximation to the motor operating point only.

Several factors could have affected the predicted efficiency with some of the mechanical losses being discussed below. Another potential loss mechanism was due to a larger air gap than previously modeled. The PCB stators were almost 20 thousandths thicker than originally intended. This required the air gap to be increased to prevent the magnets from rubbing against the stator face. This slightly larger air gap resulted in less flux between the magnet faces which could have had a small negative effect on the motors efficiency.

The reason for the larger air gap was due to this PCB consisting of design parameters (layer thickness, copper weight, pole count, etc.) that had not been built in conjunction before. Although the stator modelling software does a great job at predicting thickness based off these parameters, there was no definitive way to know the thickness until after they were produced. With each additional motor build, especially ones with different build parameters, the stator modelling software is refined to better predict board thicknesses for future builds which should mitigate concerns on PCB manufacturing performance for future projects. Even with all this considered, the additional 20 thousandths air gap would still not have had a significant impact on motor performance although it is still something that is worth controlling.

Additional losses in the motor are evident with the amount of heat generated in the inductors as seen in figure 07 in the shipboard results section. With an increase in wire temperature comes an increase in electrical resistance which would have had an additional draw on the motor efficiency. During the shipboard testing period where the data logger was recording correctly, peak temperatures on the inductors were recorded at 157 °F. However, during the motor install in Miami, FL where the ambient was close to 85 °F, these inductors were recorded to reach 210 °F which would indicate potential further efficiency losses. This was partially solved by placing the inductors over the controller cooling fan with the cooling slots facing the fan to increase airflow over them. The higher inductor temperatures were partially due to them being sized based on the false operating point. Larger inductor cores with a heavier wire gauge could have helped limit the additionally losses due to heat by reducing resistance within the wire.

As with all motors, there are areas where additional losses take place include windage, bearing drag, and flux leakage. The ECM motor was tested for this via a slightly modified generator set-up. The only change to this setup is that the stator in the ECM motor is removed to eliminate any magnetic flux interaction with the rotor and stator. The Baldor motor drove the ECM motor with no load at a range of RPM values with the torque measurements taking place at each RPM increment. This can be seen plotted in figure 09 below.

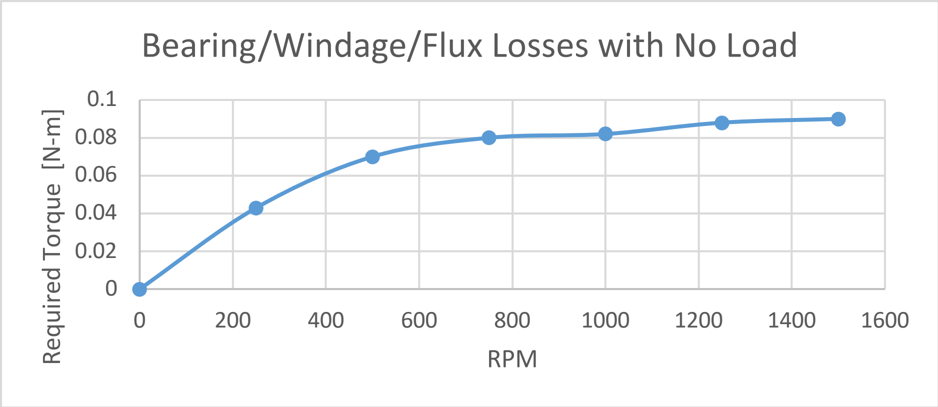

Figure 09: Mechanical Losses vs. RPM

With the increase in speed comes an increase in additional mechanical losses. In order to reduce these additional losses, a few design changes would need to be made. The most "controllable" loss would be if there was any flux leakage out the back side of the rotor. These flux lines that escaped would then interact with the motor case causing additional loss by generating eddy currents in the case. The easiest way to fix this is to use thicker back iron for the rotor to focus the flux within the air gap. ECM performs gauss measurements within the air gap to check for this. With the combination of the small air gap and high strength neodymium magnets, the average flux density within the air gap is on the order of 7.79 kilogauss. Measurements are then also taken towards the interior and exterior edge of the magnets to verify the extent to which the rotor/magnet structure is confining the flux to the gap. Upon measuring the flux density, 0.6 kilogauss of leakage was recorded meaning the rotor thickness was not thick enough. Although a simple solution, the time to re-machine these parts, set the magnets, and balance the entire assembly was not available.

Windage losses are slightly harder to control as this would require additional modelling of the flow characteristics inside the motor cavity. Due to how thin the motor is, the volume of air within the motor cavity is very small and the gap between the rotating and stationary components is within a couple thousandths of an inch. Sharp edges and rough surfaces had most likely caused turbulent flow within the motor cavity causing additional drag. Since these interactions take place within a fully assembled motor, it is difficult to diagnose problem areas without a computational fluid dynamics (CFD) analysis. This motor was the largest ECM had built to date and with larger motors comes larger relative velocities at the rotor edges which would theoretically compound these larger windage losses that the motor model may not have considered. This is one area of development that ECM continues to improve upon.

ECM typically uses shielded bearings in their motors to reduce the chance of any sand or particulates from getting in-between the bearing races and reducing bearing life. However, the shields cause higher friction and less efficient heat dissipation. Open bearings could be considered but there will always be the tradeoff between efficiency and reliability.

With the total mechanical drag recorded at 0.09 Nm @ 1500RPM, this quantity approximately reduced the total system efficiency by ¾ of a percent. This may seem small, and largely unavoidable, but any additional efficiency gain ECM could achieve provides not only a competitive edge in the electric motor market but additionally helps satisfy the motor design methodology to build more efficient motors in the future.

Project Conclusion

The ECM/MMA motor project identified several areas of improvement ECM could provide for shipboard motor applications. The main design and performance goals for this project were to minimize weight and showcase ECM's attractive form factor and PCB technology. The weight savings were truly remarkable with the motor (excluding controller & mounting bracket) resulting in a weight savings of almost 70% compared to the induction motor. The axial length was reduced almost three quarters and the radial size increase was only 23%. Based on the experience with this motor design, we identified further opportunities for weight savings.

Efficiency was also an area of potential improvement with an anticipated efficiency increase of approximately 2%. However, utilizing the standard off–the-shelf motor controller contributed to a lower realized efficiency along with the discovery of some additional losses contained within the motor itself. A faster switching controller with the ability to provide sufficient current would certainly allow for a direct comparison with the pre-existing induction motor and some additional efficiency gains with a second iteration motor built with ECM's PCB stator technology.

The motor described in this report was a drop-in replacement for the induction motor. The most efficiency and weight savings would be realized by a system design of the motor, fan, and HVAC control. For example, the ECM motor can be optimized for a fan-curve, with probable turn-down ratios taken into consideration. The ECM motor can also be made direct drive, and due to its form factor, integrated with the housing and cooled by the airstream. Benefits of this kind of design include much greater weight and space savings, reduction in parts and maintenance items, and opportunities to increase "wire to air" efficiency by a much wider margin.

References

Continental Control Systems LLC. (2011, November 30). *WattNode Pulse Installation and Operation Manual.* Retrieved from Continental Control Systems: file:///C:/Users/ecirc/AppData/Local/Packages/microsoft.windowscommunicationsapps_8wekyb3d8bbwe/LocalState/Files/S0/7/Attachments/Manual_WNB_Pulse[3670].pdf

Teco Westinghouse. (2007, February 19). *Performance Data 3 Phase Induction Motor.* Retrieved from Dealers Electric: https://dealerselectric.com/images/Motors/teco/PERF_DHP0034.pdf

Teco Westinghouse,. (2007, February 23). *Outline Dimensions 3 Phase Induction Motor.* Retrieved from Dealers Electric: https://dealerselectric.com/images/Motors/teco/OL_DHP0034.pdf

ECM
SOFTWARE & TECHNOLOGY
www.printstator.com

ECM Motor Validation and Test Report

Date: 4/10/2019

Document Revision: 4

ECM Model #: E – 2200 – 0.5k – 12

ECM Project: 17-MMA24

Stator Type: NON-STACKED

Motor Application: Fan Motor

Motor Type: Constant Speed Application, Belt Drive, Low Weight,

Feedback Method: Encoder

Controller Model: ABB ACS380R3

Additional Project Notes:

- Warm Motor Room (>25C)
- 460V 3 Phase Shipboard Power

Motor Serial # Delivered
1 – MMA24-0001

Motor Modeling Parameters	
Variable	**Design Value**
RPM	1760
Torque [N-m]	11.95
Watts In	2400
Watts Out	2200
Efficiency	91.6%
Volts	48.0
Kt [Nm/A]	0.369
Ke [Vs/rad]	0.427
Km [Nm/√W]	1.091
Thermal Safety Factor	1.4
Dry Weight Approx.[kg]	12.6

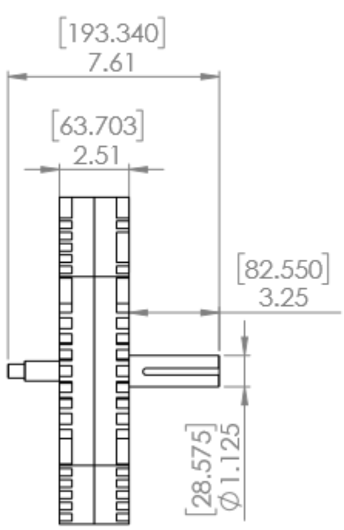

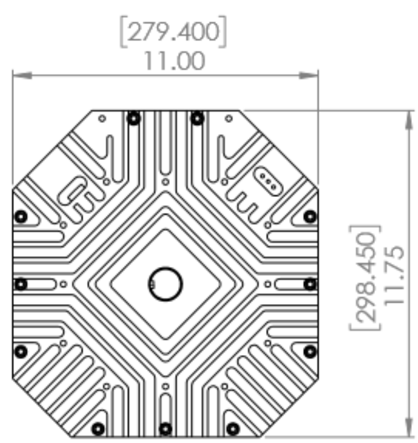

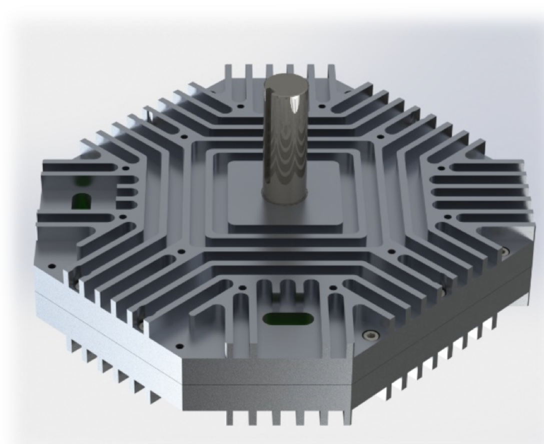

One Gateway Center, Suite 359 - Newton, MA 02458 ◆ Phone: (617) 340-3241 ◆ info@e-circuitmotors.com

COMPLIANCE TESTS

TEST	VALUE / SPEC. PER DATA SHEET	TESTED RESULT / VALUE	COMMENTS
Individual Parts Inspection and Tolerance Verification	Acceptable Tolerance Range Magnet Thickness: +/- 0.002'' Bearing Pocket Depth: +/- 0.002'' Stator Pocket Depth: +/- 0.002''	Measured Tolerance Magnet Thickness: +/- 0.002'' Bearing Pocket Depth: +/- 0.001'' Stator Pocket Depth: +/- 0.002''	
Stator Physical Inspection and Verification of Electrical Parameters Test Procedure: 5	Expected Value Phase to Phase R 1-2[mΩ]: 152.40 R 2-3[mΩ]: 152.40 R 1-3[mΩ]: 152.40	Average Recorded Value R 1-2[mΩ]: 166.11 R 2-3[mΩ]: 165.49 R 1-3[mΩ]: 165.65	Mount holes in the stator were 4-5 thousandths of an inch undersized which required post drilling operations to be performed.
Balance & Vibration Test via EI-30 Balance Machine Test Procedure: 10	<6	Average Balance Quality 0.51	Balance readings reflect balance achieved on ECM lab motor.
Air Gap Measurement & Verification Test Procedure: 6	0.2170''	Average Air Gap 0.2280''	
Gauss Testing & Gap Flux Verification Test Procedure: 8		Gauss Readings [k Gauss] Min / Max Flux Readings +/-: +7.86 / -7.84 Average Flux Readings +/-: +7.76 / -7.73	
Verify Motor Torque Constant (Kt) Test Procedure: 1, 2b	0.369 [Nm/A]	Average Kt 0.370 0.373	
Verify Motor Voltage Constant (Ke) Test Procedure: 1, 11	0.427 [$V_{l-l\,amp}$ s/rad]	Average Ke 0.428 0.421	

TEST	VALUE / SPEC. PER DATA SHEET	TESTED RESULT / VALUE	COMMENTS
Power Loss & Motor Efficiency Test Procedure: 2	| | Expected Value | | Power Loss [W] @ OP | 200.0 | | Motor Efficiency @ OP | 91.60 |	| | Generator Mode Average [1500 RPM] | Motor Mode Average [1500 RPM] | | Power Loss [W] | 206.0* | 323.0* | | Efficiency | 87.0* | 82.6* |	*Tests occurred at slower speeds due to controller not being able to reach designed operating point conditions.
Test Mechanical Losses (bearing, windage, etc.) **Test Eddy Current Losses** Test Procedure: 3	0.396 @ 1760 RPM	| | Windage, Bearing & Flux Leakage Losses [N-m] | Eddy Current Losses [N-m] | | RPM 1000 | 0.082 | 0.433 | | RPM 1500 | 0.090 | 0.637 |	
Thermal Characterization of Stator to Case Test Procedure: 7	Stator Temp < 100 °C Thermal Safety Factor: 1.4	| Stator Sticker Tripped Temperature Range [°C] | 71 – 77 | | Housing Temperature [°C] | 56.3 | | Power Loss [W] | 149.0 | | Stator to Case Heat Resistance [W/ °C] | 7.10 – 10.10 |	
Thermal Characterization Case to Ambient Test Procedure: 7	Housing Temp < 75 °C	| Ambient Temperature [°C] | 20.6 | | Housing Temperature [°C] | 56.3 | | Power Loss [W] | 149.0 | | Housing to Ambient Heat Resistance [W/ °C] | 4.20 |	The housing was cooled via natural convection in a laboratory setting. These calculated values will be inapplicable for a forced convection cooling method including but not limited to an external blower fan.
Dielectric "Hi-POT" Withstand Test Test Procedure: 8	| AC/DC Test | Minimum Allowable Voltage to PASS | | AC | >1000 V | | DC | >1000 V |	| AC/DC Test | Grade | | AC | PASS | | DC | PASS |	

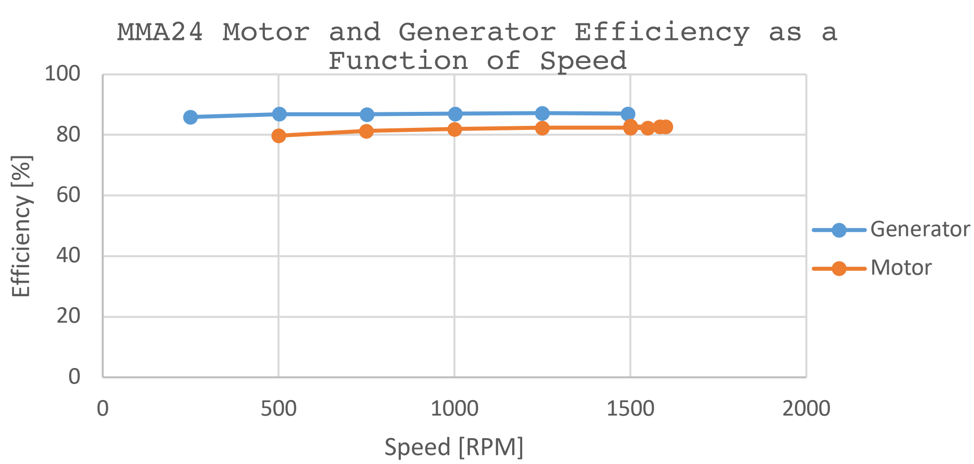

Figure 01: Speed varied while constant resistance (designed to hit operating point load and speed) applied to load motor leads in back-to-back test stand setup.

MOTOR TEST DESCRIPTIONS

1. **Spin Down Test**
   The motor is attached to a test stand, with phase voltages measured by a PicoScope 3000 data acquisition system. The motor is given an initial condition and allowed to "spin down", or decelerate, under its own losses. The data collected from this test encode the rotor position as a function of time and allow estimation of Kv, Kt and associated loss terms.

2. **Back-To-Back Setup**

   a. Two motors were coupled to one another to setup a motor-generator configuration. The setup is as follows. The Device Under Test (DUT) motor is mounted on one side of the test stand, there is an Futek TRS600 50Nm rotary torque sensor mounted in the middle then the load motor in this case was the Baldor CD6203. The motors are each attached to the sensor using SC050 flexible servo shaft couplers. The DUT was controlled by an ABB ACS380 controller to a range of speeds from 0 to 1600 rpm during which time the Baldor motor was used as a load by applying a resistor bank across the armature and then adjusting the field voltage to tune the torque to desired values.

      Power into the motor was measured using a Yokogawa WT5000 power analyzer setup in 3P3W configuration. Motor speed was measured both on the ACS380 as well as the Extech DT22401D keyed shaft tachometer. Power to the controller was supplied by 3 phase line voltage passed through a Square D transformer. Power into the controller was not recorded so system efficiency was not captured in this test. The data collected is used to motor and controller efficiencies

   b. The same test stand setup was used to collect data on the DUT acting as a generator. In this case the Baldor motor was used to drive the DUT instead of being the load. The power analyzer was used to measure power out of the DUT which was connected to a resistor bank that was setup to provide the appropriate load to the motor.
      Measurements were taken by the power analyzer, Futek torque sensor, and shaft tachometer at speeds of 0, 250, 502.4, 751.6, 1002, 1250, and 1493. These measurements allow isolating the performance of the motor without any negative effects caused by non-ideal control. The data collected here is used to calculate performance under ideal circumstances and kt.

3. **Windage**
   While in the Back-to-Back setup b using the Futek TRS600 and Baldor motor to drive the DUT, speed and torque measurements are taken while the DUT side is not connected to a resistive load. This test allows measurement of losses associated with eddy currents in the stator and case as well as windage and bearing losses.
   The motor is then disassembled to have the stator removed. At this point the rotor/shaft assembly is reassembled and put back into the case. The Baldor motor is once again used to drive this stator-less motor to speed while torque measurements and shaft speeds are recorded. This process allows windage/bearing losses and eddy current losses to be isolated from the previous measurement of both combined.

4. **Run and Tear Down**
   The motor was run through the previously mentioned testing after which it was disassembled and inspected for any problems. Possible problems to visually inspect for include bearing integrity, FOD, bearing to shaft fit, bearing to case fit, evidence of excessive temperature, evidence of arcing, evidence of stator rotation, evidence of magnet/stator interference, integrity of thermal compound, runout issues, and condition of magnets and coatings. None of the above problems were found.

5. **LCR Meter**
   Stator electrical measurements are taken using a Keysight E4980AL Precision LCR Meter. Stators are measured across the 3 connection, measuring from position 1 to 2 then 1 to 3 then 2 to 3 in order to record all possible combinations. These measurements are recorded using the Ls-Rdc profile on meter.

6. **Wedge for Gap Measurement**
   Measuring the gap between the assembled rotors is challenging due to the effects of the magnets on the tools needed for measurement. The way these effects are overcome is through using a non-magnetic wedge to make a transfer measurement. The wedge is a piece aluminum machined to have a small taper. It is inserted into the gap at several locations around the rotor and marked at the point it makes contact with the magnet surface. The wedge is then removed, and measurements are taken using Mitutoyo 293-335-30 Digital Micrometer at each of the marks that were made. This allows measurement extremes and average of the gap between the magnetic surfaces.

7. **HiPot**
   HiPot testing is done to ensure the stator does not fault to the case under extreme voltage conditions. This test is done by attaching the positive lead of GW Instek GPT-9603 to one of the motor leads and attaching the negative lead to the motor case. The HIPOT tester applies either an AC or DC voltage across its leads and measures current. The user selects the voltage applied and the current level for pass/fail. These motors were tested and passed both 1.0 kV AC 2.5 mA and 1.0 kV DC 1.0 mA.

8. **Gauss Testing**
   The rotor/shaft assembly was assembled without a stator. This assembly was then supported so the rotational axis of motor was in horizontal position while using V-Blocks on the shaft bearings so that the rotors could be spun by hand. A F.W. Bell 6010 Gaussmeter was used to measure the field in the gap between the rotors at 3 different locations as well as on the back side of the rotor. The rotor shaft assembly is then spun in a full revolution to ensure each pole is measured. The 3 locations of measurement are just inside the ID of the magnet, just inside the OD of the magnet and the center of the magnet. The field is recorded using a PicoScope to capture the data from the Gaussmeter.

This data is then analyzed to determine the average peak value at each location. When measuring the leakage on the backside of the motor the Gaussmeter is set to hold the highest value and swept all around the back to cover the entire surface. This is then repeated using hold minimum value to collect the extremes in both pole directions.

9. **Thermal**

The DUT was setup as in Back-to-Back setup b. The Baldor motor drives the shaft of the DUT while a 3-phase resistive load bank is attached across its terminals. Prior to mounting the DUT for the test it is disassembled and has Telatemp and Thermax temperature stickers placed on the inner end turn of the stator. These stickers come in a variety of temperature ranges and are designed to trigger a specific section of the sticker when the given temperature has been reached. The motor is then reassembled and setup in the test stand.

A thermocouple is attached to the motor case to monitor temperature of the case during the test process. The test is now ready to begin. The Baldor motor is used to drive the shaft of the DUT to desired speed. The initial case temperature, ambient temperature, torque on shaft, speed, power to resistor bank and start time are recorded. These measurements are repeated approximately every 15 minutes until the DUT case reaches steady state or desired length of time has passed, in this case the test was done for 2 hours. At the end of the test measurements are recorded a final time.

The motor is then disassembled, the stickers are viewed to determine the highest temperature the stator reached. This value then gives you a range of possible temperatures reached because there is a highest reached and the next temperature that was not triggered. The stator reached some temperature in between these 2 values. The data collected here is used to calculate thermal resistance from the stator to case as well as the case to ambient within a small range. The thermal resistance values allow estimation of the stator temperature based off temperature of the case.

10. **Balance Machine**

An Erbessd dynamic balancer is used to balance the rotor assembly. If needed, corrections can be made by adding or subtracting masses at a prescribed radius. To balance the rotor, the stator is removed, and the bearing, shaft and rotors are spun up. A laser system measures speed, accelerometers detect the imbalance, and the degree of balance and location of corrective mass is calculated by the instrument.

11. **BACK EMF**

The Device Under Test (DUT) motor was fixtured in a test stand such that it was rotated at constant speed using a Baldor CD6203 to drive the shaft of the DUT. The unloaded phase voltages were measured at 0, 250, 500, 750, 1000, 1250, 1500, 1750 RPM using a Yokogawa WT5000 power analyzer. Speed was recorded using an Extech DT22401D keyed shaft tachometer. These speeds and voltages are processed by an Octave script to confirm the motor kV value.

Testing Image (Back to Back Set Up)

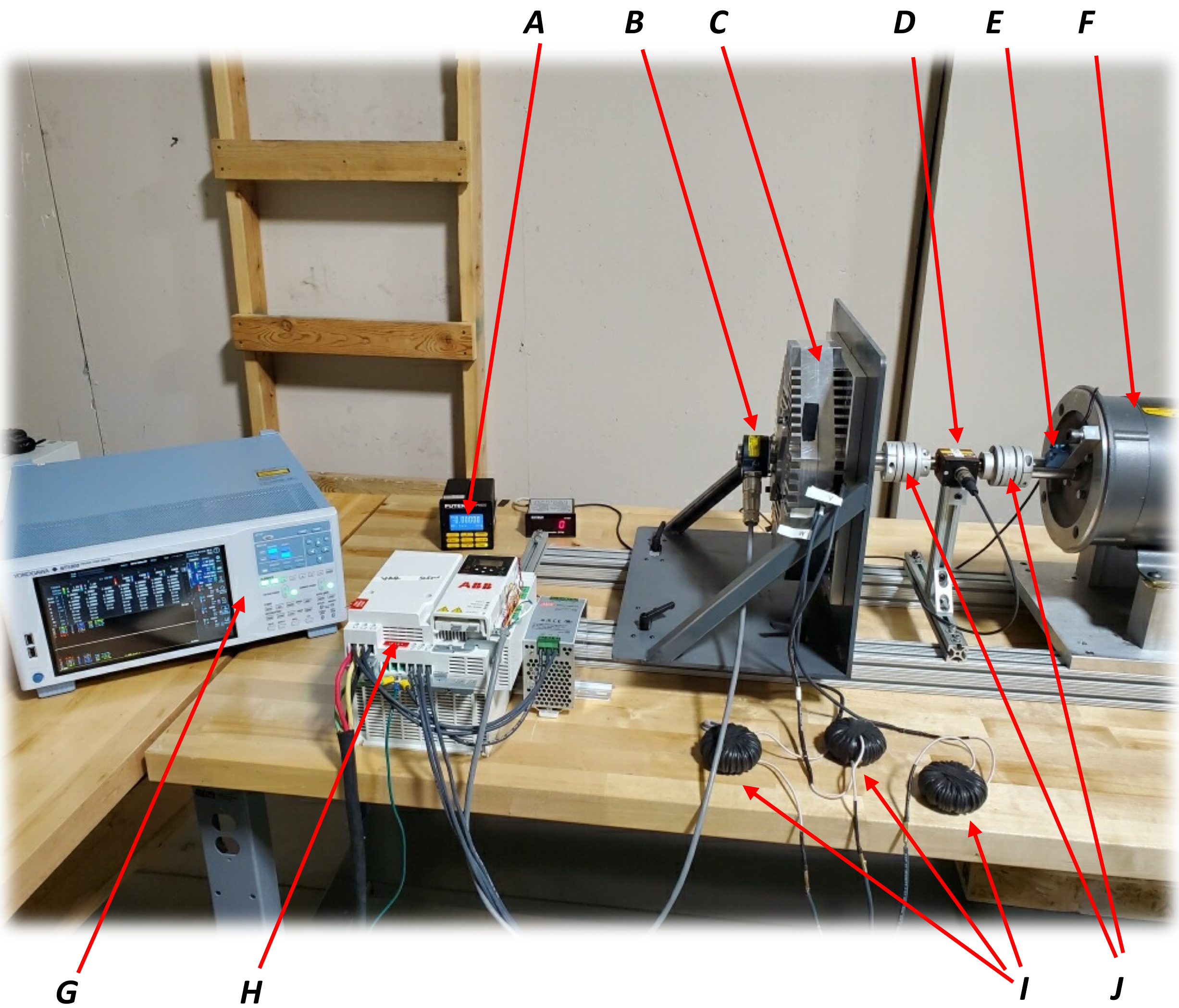

Letter	Test Component
A	Futek Display Screen
B	BEI DS0514 Shaft Encoder
C	ECM Generator/Driving Motor
D	Futek TRS600 50Nm torque sensor
E	Shaft Tachometer
F	Baldor Generator/Driving Motor
G	Yokogawa WT5000 Power Analyzer
H	ABB ACS380 Controller
I	Inline Inductors
J	Shaft Couplings

STATEMENT OF MATURITY

Client Name: E-Circuit Motors
Date Issued: 10 June 2019

Certificate Number: T1872420

Operationally Qualified

This is to certify that

E-CIRCUIT MOTORS PRINTED STATORS FOR MOTOR APPLICATIONS

has been reviewed in accordance with the ABS *Guidance Notes on Qualifying New Technologies*. The technology has been performing its intended functions in service, in accordance with the defined performance requirements as outlined in the System Requirements and Description Document.

Description and Application:

E-Circuit Motors (ECM) utilizes its software to "print" stators which can be used in many types of electric motors and generators. ECM's technology eliminates the need for wire winding and iron laminations used in conventional motors and generators, by embedding copper-etched conductors into a multi-layered printed circuit board to form a stator that works in conjunction with permanent magnets

ECM selected a 3 HP Air Handler induction motor on the MMA Training Ship "T/S KENNEDY for this project. ECM developed a Printed Circuit Board (PCB) stator motor which would replace the 3 HP Air Handler motor on-board in order to evaluate performance between the base line Induction Motor and the PCB Motor.

The compiled results and analysis were submitted by ECM and it is determined that the PCB motor provides significant reduction in weight and space saving along with an increase in performance. As indicated by ECM the performance aspects can be improved through the selection of motor controllers for the specific application and upgrades to the equipment.

The PCB Motor Installation is comprised with the components listed below:

- Printed Circuit Board Motor
- BEI DS0514 Shaft Encoder
- Commercial off the Shelf (COTS) Motor Controller – ABB ACS380

Boundaries:

The Commercial off the Shelf (COTS) Motor Controller – ABB ACS380 was not included within the scope of the technology qualification as this equipment does not introduce any novel elements. The qualification is limited to a 3 HP PCB motor or smaller for non-essential applications. Scalability and applications exceeding this limit are subject to review and surveyor witnessing.

Scope of Review:

1. **Engineering Review**
   ECM submitted the original design package of the PCB motor to ABS Engineering. The initial review of the drawings, documentation and New Technology Qualification plan was completed to the applicable sections of the ABS Rules for Building and Classing Steel Vessels, 2019 and the ABS Guidance Notes on Qualifying New Technologies, 2017. This review covered the Feasibility and Concept Verification Stages under the New Technology Qualification Process.

ABS Global Engineering\
1701 City Plaza Drive | Spring, TX 77389 USA

2. **Manufacturing Facility Survey**
ABS surveyor attended the Prototype Testing for the electrical motor (E-2200-0.5K-12) at the Bozeman Facility in Montana for the Prototype Validation Stage under the New Technology Qualification Process. The surveyor witnessed the Motor Run under load test. The remaining tests were conducted by the manufacturer and the test results were submitted to engineering for review.

Prototype Test Schedule:
 a. Individual Part Inspection and Tolerance Verification
 b. Stator Physical Inspection and Verification of Electrical Parameters
 c. Balance and Vibration Test
 d. Air Gap Measurement & Verification
 e. Gauss Testing & Gap Flux Verification
 f. Verify Motor Torque Constant
 g. Verify Motor Voltage Constant
 h. Power Loss & Motor Efficiency
 i. Test Mechanical Losses
 j. Thermal Characterization of Stator to Case
 k. Thermal Characterization of Case to Ambient
 l. Dielectric “Hi POT”: Withstand Test

3. **Ship Installation Survey**
ABS surveyor attended the "T/S KENNEDY", Class No. 6704200, at Buzzards Bay, Massachusetts, in order to examine and report on the installation of the PCB Motor as part of Integration Stage under the New Technology Qualification Process.

- One (1) prototype printed circuit board permanent magnet synchronous electric motor (ECM Model # E- 2200-1.8k-12, Serial # MMA24 0001) was installed on the Air Conditioning “A” Supply Fan No. 01-139-2, located in the Upper Deck Fan Room (Port, Inner, Frames 138 - 145) via a double-v groove pulley belt drive. The motor was installed and commissioned by ECM Personnel.

- The installation included a Variable Frequency Drive, Inductor, Shaft Encoder and Data Logger.

- A review of the data logger files indicated continuous operation from 16 February 2019 through 6 March 2019.

- The following data was demonstrated at the time of attendance:
  - Drive Speed: 1500 rpm
  - Motor Casing Half Temperature (Encoder Side): 119.788 °F
  - Motor Casing Half Temperature (Drive Side): 126.354 °F
  - Fan Room Relative Humidity: 11 %
  - Fan Room Temperature: 72.739 °F
  - Inductor Enclosure Temperature: 147.157 °F
  - Kilowatt-Hours: .003 kWH

4. **Motor Validation and Test Report and Lab Testing Report**
ABS Engineering received the Prototype Test Survey Report, On-Board Installation Survey write-up, finalized test reports from the Prototype Tests and the Lab Testing Report for the PCB Motor. The Lab Testing Report analyzed the results from the motor during the system integration stage. ABS evaluated these documents along with the original engineering submission and concluded that this technology is Operationally Qualified under the New Technology Qualification Process subject to the recommendations/comments that were identified in this document.

Comments/Notes:

1. Each installation is to be submitted to ABS for review and is to include at minimum the following drawings:
   a. Vessel Installation Arrangement Drawings
   b. Power and Control Connection Drawings
   c. Forced Cooling/Ventilation Drawings, if applicable
   d. Complete Bill of Materials (e.g. Cable Details, Motor Controller, etc.)
   e. Motor Controller Schematic Drawings

Reference Documents:
See Attached List

ABS shall in no event be held liable for any identified/unidentified hazardous scenarios or qualification activities associated with this technology.

Roy H. Bleiberg
Vice President, Engineering

Electronically Signed by: Anju Valookkaran

Documents List

No.	Rev. No.	Rev. No.	Title	Status
1	S3608109	-	Surveyor Report	Reviewed
2	Surveyor Report	-	Installation Survey Report	Reviewed
3	ECM Test Plan	-	ECM Test Plan	Reviewed
4	Installation Pictures	-	Installation Pictures	Reviewed
5	ECM - MMA FMEA	3	TS KENNEDY FMEA	Reviewed
6	ECM and MMA ABS Report	5	ECM and MMA ABS Report	Reviewed
7	E CIRCUIT MOTORS Survey Installation Report	-	E CIRCUIT MOTORS Survey Installation Report	Reviewed
8	P170001	1	MMA24 Stator Outline	Reviewed
9	400 series HALT 30 G	-	Core Motion's 400 Series, Vibration Test	Reviewed
10	400 series HALT 50 G	-	Core Motion's 400 Series, Vibration Test	Reviewed
11	P170003	4	MMA 24 Rotor	Reviewed
12	A170029	9	BEI Encoder Hub Shaft	Reviewed
13	P170005	9	BEI Encoder Shaft	Reviewed
14	P170002-00	2	Magnet Grade N42H MMA 24	Reviewed

15	FAQS	-	Frequently Asked Questions - E-Circuit Motors	Reviewed
16	A180004	A	ECM/MMA Motor Integration	Reviewed
17	Haltmotor2Vibration	-	Core Motion's 400 Series, Vibration Test	Reviewed
18	ACS380 Datasheet	-	Low Voltage AC Drives ABB Machinery Drives ACS380	Reviewed
19	Haltmotor1ThermalShock	-	Thermal Shock and Ramp	Reviewed
20	P170014	6	MMA Case Back	Reviewed
21	MMA32	-	ECM Motor Datasheet E-2200-1.8k-12	Reviewed
22	P170029	2	Hub Pre Assembly	Reviewed
23	22 layer	-	Cover Letter PCB Motor	Reviewed
24	P170015	6	MMA Case Front	Reviewed
25	StatorOverlaymma32	-	Overlay MMA32	Reviewed
26	ECM TQM	-	Summary of ECM quality, H,S and Env 12	Reviewed
27	31057H379001	-	Outline Dimensions 3-Phase Induction Motor	Reviewed
28	SRDD V1	-	ECM E-Circuit Motors System Requirements and Description Document	Reviewed
29	ECMMMA Installation Introduction	-	ECMMMA Installation Introduction	Reviewed
30	P170012	1	Hall Board MMA 24	Reviewed
31	A170002	2	MMA 24 Assembly Drawing	Reviewed

The Potential Contribution of Light-Weighting to Reduce Transport Energy Consumption

Hinrich Helms* and Udo Lambrecht

Institute for Energy and Environmental Research (IFEU) Heidelberg, Wilckensstr. 3, 69120 Heidelberg, Germany

* **Corresponding author** (Hinrich.Helms@ifeu.de)

DOI: http://dx.doi.org/10.1065/lca2006.07.258

Abstract

Background, Goal and Scope. The transport sector contributes significantly to the global energy consumption and greenhouse gas emissions. Among other measures, also light-weighting of vehicles is discussed as a way to reduce the energy consumption and, thus, also CO_2 emissions of transport. Currently, most Life Cycle Assessments (LCAs) use rough estimates on potential energy savings by light-weighting, which are not comparable due to different scopes and methodologies. This paper therefore presents a set of scientific data for use phase energy savings for different vehicle types for a harmonised and, thus, comparable weight reduction of 100 kg.
Road and rail vehicles, ships and aircrafts are covered in this paper. Besides an analysis on a per vehicle basis, the potential contribution of light-weighting to a reduction of the global transport energy consumption is also estimated. All analysed energy savings are independent of the technical realisation of the weight reduction (e.g. new materials or improved design or logistics). The data can therefore be used in LCAs of different light-weighting technologies.

Methods. Available data have been analysed in respect to system boundaries and methodologies. Several sources which are suitable for a comparable quantification of specific energy savings per vehicle-km or the use phase energy savings, for example, have been identified. In order to obtain more differentiated data and close the data gaps, specific modelling has also been undertaken for articulated trucks. Data have been checked for plausibility against the analysis of physical resistance factors and been converted to a harmonised and, thus, comparable weight reduction of 100 kg.

Results and Discussion. The energy consumption per vehicle-km depends largely on the physical resistances which the vehicle has to overcome during its operation. Ground vehicles operated in urban areas, with frequent stops and accelerations, are generally capable of higher energy savings for a given weight reduction compared to vehicles on highways at steady speeds. The total use phase energy savings for a 100 kg weight reduction also depend on the total use phase transport performance. Road vehicles realise about the lowest use phase energy savings due to the limited use phase mileage. Rail cars commonly have a higher use phase mileage and can therefore achieve higher use phase energy savings. Even higher savings are estimated to be achieved by a weight reduction of high-speed ferries (about 10 times higher compared to rail vehicles) and aircraft (about 100 times higher compared to rail vehicles).

On a global level, however, road vehicles and especially passenger cars could make the highest contribution to reduce energy consumption by light-weighting. This is due to the high share of these vehicles on the global energy consumption (because of the huge number of these vehicles) and also a considerable potential to realise a further weight reduction.

Conclusion and Perspectives. Light-weighting is one way of reducing transport energy consumption in the use phase. The differences in use phase energy savings for a 100 kg weight reduction between the vehicle groups are considerable and allow for the identification of priorities for future light-weighting efforts. The contribution to a reduction of the global transport energy consumption, in turn, depends on the further potential for a weight reduction and on the number of vehicles which can be weight reduced. The OECD market of private passenger cars and trucks, for instance, offers a good perspective due to a high contribution to the global transport energy consumption, a considerable potential for weight reduction and a high turnover rate of the vehicle fleet. The benefits will be realised after a substantial replacement of the existing fleet with new, weight-reduced vehicles.

Keywords: Aircraft; articulated trucks; carbon dioxide; energy savings; ferries; light-weighting; passenger cars; trains; transport; weight reduction

Introduction

The transport sector contributes significantly to the global energy consumption and greenhouse gas emissions, and still experiences high growth rates. According to the International Energy Agency (IEA), almost one quarter of the global energy production is consumed by transport (IEA 2003a, IEA 2003b). This is a call for action for the transport sector to find ways to save primary energy resources and reduce greenhouse gas emissions. For passenger cars, for instance, the European Automobile Manufacturers Organisation (ACEA) has already made a commitment to reduce the specific CO_2 emissions of new passenger cars to 140 g per km until 2008.

The reduction of the weight of transport vehicles is discussed as one way to reduce the energy consumption and, thus, CO_2 emissions caused by the transport vehicles. Not only the physical energy demand, but also the energy consumption associated with upstream processes, such as the extraction and processing of fuels and electricity, as well as the distribution and conversion into mechanical energy, is reduced.

Currently, different estimates are used to calculate energy savings by light-weighting which are not always scientifically robust and are often not comparable due to different system boundaries and methodologies. This paper therefore presents a set of scientific data for use phase energy savings for different vehicle types for a harmonised and, thus, comparable weight reduction of 100 kg. Such data can be used for a comparison of light-weighting in different vehicles, adapted for the use within LCAs of different light-weighting options such as new materials or improved design and also for logistic analyses.

This article presents primary energy savings to allow for a better illustration and comparison between vehicle types with different energy carriers. As an Annex, an overview of suggested average 'end energy' savings is also presented. These data allow for a use in LCAs with different energy splits, efficiencies of power generation and CO_2 emission factors.

1 Scope

The spectrum of vehicle types covers road (passenger cars and articulated trucks) and rail vehicles (subways and intercity trains) as well as high-speed ferries and aircraft. Since these vehicles use different energy carriers, primary energy savings have been calculated for each vehicle type. Primary savings are calculated based on data for the EU15 from various sources which are documented in previous IFEU studies (IFEU 2003, IFEU 2004). The extraction and processing of fuels and electricity as well as the distribution and conversion into mechanical energy is thus included in these values.

The focus is on the use phase, which covers the whole operational life of the vehicle. The means by which the weight reduction is technically realised, e. g. by the use of light-weight materials, is not considered. Production of materials, as well as material scrappage or recycling, is thus not included in the system boundaries.

The use phase energy savings for the defined weight reduction of 100 kg at a defined vehicle depend on a range of use characteristics. The vehicle characteristics and its use pattern can be distinguished from the use phase performance (e.g. vehicle-km) (**Table 1**). Only the consideration of both allows for an assessment of potential use phase energy savings. For the total potential for energy savings by light-weighting, fleet characteristics also have to be considered (see Table 1).

Energy savings are thus analysed at three different levels using different reference bases:

a) Specific energy savings per weight reduction (100 kg) and vehicle-km (100 km) for different vehicle types. These savings depend on the technical and operational characteristics of vehicles.
b) Use phase energy savings for a weight reduction of 100 kg. These savings depend on the use intensity and life-time of the vehicles.
c) The potential reduction of the global transport energy consumption by a weight reduction of different vehicle groups. This reduction potential also depends on the specific potential for a weight reduction of different vehicles and their global annual energy consumption.

2 Methodology and Background

This analysis first considers the physical resistance factors for ground vehicles which determine the relation between vehicle weight and energy consumption. Afterwards, available estimates and measurement data for ground vehicles, and also for aircraft and high-speed ferries, have been analysed in respect to system boundaries and methodologies. Several sources which are suitable for a comparable quantification of, for instance, specific energy savings per vehicle-km or the use phase energy savings have been identified. In order to obtain more differentiated data and close data gaps, specific modelling also has been undertaken for articulated trucks. All data have been checked for plausibility against the analysis of physical resistance factors and been converted to a harmonised and, thus, comparable weight reduction of 100 kg.

Generally, energy consumption of vehicles is due to the physical resistance factors which the vehicle has to overcome during its operation. The resistance factors and thus energy savings by light-weighting vary by vehicle type. For the dominating ground vehicles (road and rail vehicles), the main resistance factors are:

- Rolling resistance (proportional to mass and rolling friction)
- Gradient resistance (proportional to mass and gradient)
- Acceleration resistance (proportional to mass and acceleration)
- Aerodynamic resistance (proportional to vehicle dimensions and speed)

With the exception of aerodynamic resistance, all resistance factors for ground vehicles are linearly dependent on the mass of the vehicle. The aerodynamic resistance, however, depends on the dimensions of the vehicle and the square of speed. With the same driving situation and behaviour as-

Table 1: Factors of influence on energy savings by light-weighting

	Use phase energy savings		Global potential for energy savings	
	Vehicle and use characteristics	Use phase performance	Potential for weight reduction	Energy consumption of the fleet
Factors	• Use pattern (driving cycle) • Driving behaviour • Vehicle resistance • Well to tank efficiency • Tank to wheel efficiency • etc.	• Use intensity (h or km per year) • Durability of vehicle • Climate • Overhauling of vehicles • etc.	• Current use of light-weight materials • Economic and political facilitation • Consumer choice • etc.	• Number of vehicles • Use intensity of vehicles • Specific energy consumption of vehicles • etc.

sumed, the correlation between energy consumption and vehicle weight is therefore linear (Ehinger et al. 2000, Eberle and Franze 1998). Therefore, the absolute energy savings for a 100 kg weight reduction in the same driving cycle and with the same technical specifications are 'not depending on the vehicle's weight level' (Eberle and Franze 1998). This fact ensures that results for a 100 kg weight reduction are also comparable between ground vehicles with very different gross weights (e.g. passenger cars and trains).

Besides the vehicle characteristics (dimensions, mass), driving and road characteristics such as speed, acceleration and road gradients also determine the energy consumption. For ships and planes, other resistance factors have to be considered. Aerodynamic resistance plays a major role for aircraft, while water resistances dominate for ships. The energy consumption of ships is therefore related to the ship's displacement, thus also the ship's weight. Despite this complexity, selected data sources for aircraft and a high-speed ferry have been included in order to allow for a comparison between the different vehicle types.

The potential contribution of light-weighting to reduce the transport energy consumption also depends on the weight reduction potential and the total energy consumption of different vehicle groups. This total potential energy savings by a light-weighting of different vehicle groups has been calculated in a top down approach based on figures on the global transport energy consumption for the year 2000 (IEA 2003a, IEA 2003b). Energy savings by light-weighting have afterwards been applied to this baseline energy consumption.

3 Results for Different Vehicle Types

3.1 Passenger cars

The term 'passenger cars' covers a broad range of vehicles from compact cars with less than 800 kg to vehicles with more than 2,500 kg vehicle weight. The weight of the growing numbers of Sport Utility Vehicles (SUV) can be even higher than 2,500 kg. Furthermore, for the use phase mileage, private and commercial vehicles have to be distinguished. Commercial vehicles (e.g. taxis, company cars) generally have a much higher annual mileage compared to private vehicles.

The estimates for fuel savings per 100 km for a 100 kg weight reduction range from 0.15 to 1 l per 100 km for a 100 kg weight reduction (IFEU 2003, Eberle 2000) and can therefore affect the total results of an LCA significantly. This, in turn, has an influence on political and economical strategies. Most of these estimates, however, lack a scientifically chargeable and practically approved basis and depend on the specific interests involved (Eberle and Franze 1998). Data from scientific tests and simulations should therefore be preferred.

In a comprehensive PhD thesis on this topic, fuel savings have been tested and simulated with and without an adjustment in the rear axle transmissions to the new power to weight ratio (Eberle 2000). Weight induced fuel savings with adjusted rear axle transmission (0.41 l/(100 km*100 kg)) turned out to be about three times higher as that for vehicles without adjustments (0.13 l/(100 km*100 kg)). Light-weighting could therefore be one important measure towards meeting the ACEA targets for 2008. For an estimate of use phase energy savings, data which take into account the adjustments in the rear axle transmission are used, because new passenger cars will be optimised for their current power to weight ratio. Furthermore, in principal, a weight reduction also allows for downsizing of other components (weight spiral) which are not considered here.

Simulation values for fuel savings in the New European Driving Cycle (NEDC) with adjustments in the rear axle transmission range from 0.34 to 0.48 l/(100 km*100 kg) for gasoline cars can even reach 0.510 l/(100 km*100 kg) in case of sportive driving (Eberle 2000). A similar level of fuel savings is also indicated by other sources, e.g. (Schmidt et al. 2004): 0.38 l/(100 km*100 kg). Fuel savings for diesel vehicles turn out to be slightly lower, in the range of 0.29 to 0.33 l/(100 km*100 kg) in the NEDC (Eberle 2000).

200,000 km is a widely accepted use phase performance for average private passenger cars in Europe as well as the US (Reppe et al. 1998, Ridge 1997, Kelly and Davis 1998). Special vehicles (e.g. taxis or company cars), however, can have a much higher annual performance and are therefore assumed to have a use phase mileage of up to about 800,000 km for exemplification.

Thus, primary energy savings for a 100 kg weight reduction vary significantly for the defined vehicles. Average private passenger cars range between 25 GJ (Diesel) and 27 GJ (Gasoline). Much higher use phase energy savings can be achieved by a high performance taxi (115 GJ), mainly due to the higher use phase mileage, but also higher specific energy savings due to the more dominant urban use.

Passenger cars are estimated to have consumed about one third of the global transport energy consumption (30 million TJ) in 2000 (IEA 2003a, IEA 2003b). This makes passenger cars the dominant vehicle group in transport energy consumption. Since the weight of private passenger car new registrations in the OECD countries has not decreased much in recent years, a considerable potential for further weight reduction can be assumed. For the use of aluminium, for instance, a potential for a further weight reduction of a state-of-the-art passenger car by about 7% has been identified by (FKA 2002).

3.2 Articulated trucks

For articulated trucks, direct energy savings (fuel savings by lighter vehicles) and indirect energy savings (fuel savings by a higher payload) are distinguished. Indirect energy savings, however, will only occur in the case of weight limited cargo and refer to the energy consumption per t-km.

Due to the limited availability of data on fuel savings by light-weighting for articulated trucks, a consistent set of fuel consumption data has been modelled (see IFEU 2005). The modelling has been undertaken for a 40 t maximum gross weight truck by using the 'Passenger car and Heavy duty vehicle Emission Model' (PHEM) which has been developed by the Graz University of Technology (see (Hausberger et al. 2002) for a detailed model description). The model takes into account differentiated engine maps derived within the

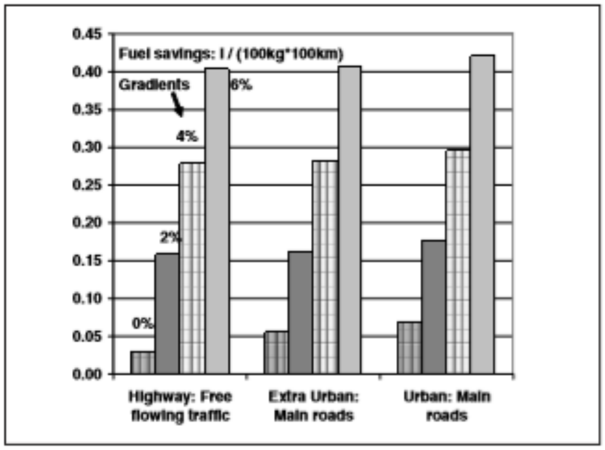

Fig. 1: Fuel savings for articulated trucks in different traffic situations and for different gradients

European ARTEMIS project and uses 'real world' driving cycles which are based on over 30,000 km of speed profiles which have been recorded using the car-following method. The fuel consumption with different vehicle weights, driving cycles and road gradients has been calculated.

As expected, the fuel consumption is much higher in 'stop and go' as well as in 'urban dense' traffic. High specific fuel savings can therefore be expected in the urban environment due to frequent stops and accelerations. Fuel savings on a flat highway are about 0.03 l per 100 km for a 100 kg weight reduction, but can be up to over 0.1 l/ (100 km*100 kg) in urban traffic situations, due to frequent accelerations.

Fuel savings are also much higher on uphill roads: For a 2% gradient on a highway, fuel savings are about 5 times higher, for a 4% gradient almost 10 times higher compared to the level road. For downhill roads, no significant change in weight induced fuel savings has been found (**Fig. 1**).

In order to derive average fuel savings for articulated trucks, the differentiated fuel savings data have been weighted according to the average mileage shares for the traffic situation and gradients in Germany (TREMOD 2005). Germany has been selected due to its central location and shares of mountainous, hilly and flat roads. Average fuel savings for articulated trucks turn out to be about 0.06 l per 100 km for a 100 kg weight reduction.

Articulated trucks are mainly used in international long-distance transport and usually have a very high annual and life-time mileage. Under the assumption of a use phase mileage of 1.2 million km, use phase primary energy savings for 100 kg weight reduction turn out to be about 30 GJ, which is even higher as estimated for average private passenger cars. The high total savings are mainly due to the very high use phase mileage of articulated trucks.

If a weight reduction permits the transportation of a higher payload, less vehicle-km are needed to transport a certain amount of goods. Therefore, not the energy consumption due to weight dependent resistance factors is reduced, but the total energy consumption for the reduced transport-km. Energy savings by a weight reduction can therefore be up to three times higher compared to direct fuel savings (IFEU 2003).

Articulated trucks are estimated to have consumed about 10% of the global transport energy consumption (9 million TJ) in 2000 (IEA 2003a, IEA 2003b). Fuel consumption for articulated trucks can be considered as one cost factor; but fuel savings efforts have instead been targeted towards engines and not the full vehicle. The potential for an additional weight reduction is therefore estimated to be in the range of 1.5 t (RWTH 1999).

3.3 Rail vehicles

Rail vehicles vary much in operation pattern, length and total weight. Energy savings by light-weighting are therefore often assessed as relative benefits for a 10% weight reduction. Only few tests and simulations have been carried out with a special focus on energy savings by light-weighting of rail vehicles (e.g. Büttner 1998, Büttner and Heyn 1999, Ehinger et al. 2000). Again, weight turns out to be more important for trains with frequent stops.

Data on energy savings by light-weighting for subways or other urban trains are therefore on the high end of the spectrum and range between 6.6% (Büttner and Heyn 1999) and 8.6% (Ehinger et al. 2000) for a 10% weight reduction. High-speed passenger trains are on the low end of the spectrum (3.2% according to (Büttner and Heyn 1999)), due to their high and steady speed.

Data are also available for the weight-dependent energy consumption of normal, long-distance passenger trains, e.g. the 'Sauthoff Formula' of German Railways (DB AG 2002). From this formula, relative energy savings for long-distance passenger trains can be estimated in the range of 4% for a 10% weight reduction. This value is slightly higher than for high-speed trains, but still considerably lower as for short-distance trains. These data have been normalised to energy savings per 100 km for a 100 kg weight reduction by using data on the gross weight specific energy consumption of different train types (see (IFEU 2003)).

Further differences can be expected in respect to the use phase performance. The use phase mileage for intercity trains is estimated to be much higher (up to almost 10 million km according to (INFRAS 1999)) compared to subways or other urban trains (up to 4 million km according to (Büttner and Heyn 1999)). Using conservative values of 8 million km use-phase performance for the long-distance train and 3 million km for the urban train, use phase primary energy savings for a 100 kg weight reduction turn out to be almost twice as high for the urban trains (about 130 GJ) compared to intercity trains (about 70 GJ) (IFEU 2003). This is due to the much higher energy consumption per vehicle-km of the urban trains, to which weight-dependent resistance factors also contribute a higher share compared to long-distance trains.

Freight trains are estimated to have use phase energy savings comparable to intercity trains, but will, as for articulated trucks, offer the possibility of indirect energy savings by way of a higher payload. High-speed passenger trains (e.g. ICE, TGV) are expected to have a very high use phase mileage (up to 15 million km according to (INFRAS 1999)) and can therefore achieve higher use phase energy savings compared to normal intercity trains.

Rail vehicles have a much lower share of the global transport energy consumption compared to passenger cars. All rail vehicles combined have consumed only about 4% of the global transport energy consumption in 2000 (IEA 2003a, IEA 2003b). Some state-of-the-art rail cars already use large quantities of light-weight materials and will therefore have only a low feasible potential for further weight reduction. For steel trains, the remaining potential for weight reduction will be much higher.

3.4 Aircraft

The fuel consumption of an aircraft is heavily dependent on its weight. In fact, the fuel itself makes up a major part of the aircraft take off weight. The aircraft will constantly be losing weight during the flight; the specific fuel consumption will thus be constantly changing. As an additional effect of a weight reduction of the aircraft itself, higher weight savings will be achieved in respect to the take off weight, because less fuel has to be carried. This makes an estimate of energy savings too complex in order to be expressed as a simple coefficient. To allow for a comparison with a weight reduction of other vehicle types, an estimate has been undertaken based on airline experience.

A 'weight manager' has been developed by Lufthansa AG to calculate the fuel consumption and weight relationship. Use phase energy savings are estimated based on data from this tool (Lufthansa AG 2003) and an assumed operational use phase of 30 years. The use phase primary energy savings for a 100 kg weight reduction of short-distance planes are in the range between 10 and 20 TJ, and in the range between 20 and 30 TJ for long-distance aircraft. Planes in a long-distance flight pattern show higher use phase energy savings due to their higher number of hours in the air and, thus, higher total fuel consumption.

Use phase energy savings for a 100 kg weight reduction of aircraft can thus be expected to be over 100 times higher than for rail vehicles. This is due to the very high, mostly weight-related energy consumption and the use intensity of commercial aircraft.

Aircraft are estimated to have consumed almost 13% of the global transport energy consumption (11 million TJ) in 2000 (IEA 2003a, IEA 2003b). Many aircraft have already been optimised for weight. The potential for a further weight reduction will therefore be rather limited. On the other hand, weight savings for aircraft are particularly effective and further weight savings in respect to the take off weight also occur due to less fuel being carried. A weight-reduced aircraft hull of an Airbus A320, for instance, leads to a reduction of the take off weight by 4% (FZKA 2003).

3.5 High-speed ferries

Ships face resistance factors which are very different from ground vehicles. Energy savings by weight reduction can therefore not be expressed as a simple coefficient. A ship mainly experiences resistance from the water it is moving through. The water resistances are linked to the ships weight via the ships displacement. Furthermore, the required power is dramatically turning upwards with higher speeds. Especially high-speed ferries therefore consider light-weighting technologies.

Use phase energy savings of high-speed ferries can be exemplified by using data on the annual energy consumption from a life-cycle analysis of three different ferries using different light-weight materials (KTH/ ETH 2002). In this case study, the total engine power of the lighter versions has been adjusted to the new weight; the power to weight ratio has thus been maintained. The use phase primary energy savings turn out to be in the range of 1,600 GJ for a 100 kg weight reduction, which is about ten times higher if compared to rail vehicles, but considerably lower as for aircrafts. High-speed ferries can achieve these high absolute savings due to the high specific fuel consumption.

On a global scale, the energy consumption of high-speed ferries can be neglected. Nevertheless, light-weighting of high-speed ferries can be an important measure on a local scale.

4 Discussion of Results

A comprehensive overview has been given on use phase energy savings for different vehicles. On the vehicle-km specific level of ground vehicles, especially urban use and roads with uphill grades lead to high energy savings for a 100 kg weight reduction. Use phase energy savings, in turn, are mainly determined by the use phase mileage, which seems to be generally higher for commercial vehicles and also higher for rail vehicles in comparison with road vehicles (**Fig. 2**). Therefore, private passenger cars achieve about the lowest, urban trains about the highest use phase energy savings for a 100 kg weight reduction among the ground vehicles.

Light-weighting of high-speed ferries and aircrafts can lead to much higher energy savings, due to their very high energy consumption. It has to be noted, however, that ships and aircraft face resistance factors which are entirely different from ground vehicles. Energy savings by weight reduction are therefore not necessarily linear and cannot be expressed as simple coefficients. The values are derived from specific case studies and have been converted to the comparable weight reduction of 100 kg. Within limits, these values thus allow for a comparison with a weight reduction of ground vehicles.

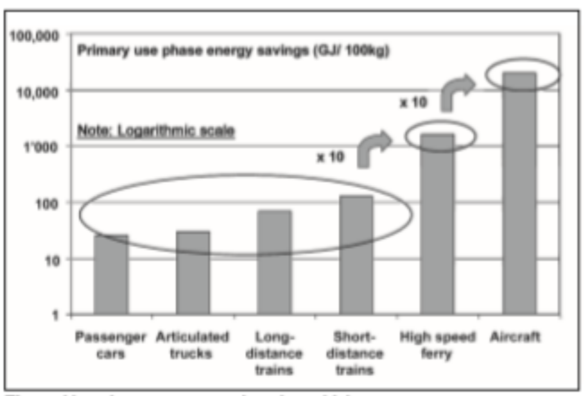

Fig. 2: Use phase energy savings by vehicle group

Three different groups in terms of order of magnitude for use phase primary energy savings can be identified. To allow for a visual comparison, aggregated vehicle groups have been plotted on a logarithmic scale.

- The gross of the considered vehicle (mainly road and rail vehicles) show use phase energy savings in a similar range.
- High-speed ferries show about ten times higher energy savings if compared, for example, to rail vehicles. This is due to the high specific energy consumption and, thus, higher potential energy savings.
- Aircraft again show about ten times higher energy savings compared to high-speed ferries and, thus, about 100 times higher energy savings compared to most ground vehicles. This is due to the very high specific energy consumption and use phase performance.

As an application of the presented data, the total global potential for energy savings by light-weighting in the transport sector has been estimated. Besides the specific energy savings for a 100 kg weight reduction, also the potential for weight reduction and the total energy consumption of the respective vehicle group has been taken into account. These factors differ considerably between the vehicle groups.

The total energy consumption of different vehicle groups in different world regions in 2000 (IEA 2003a, IEA 2003b) is used as the baseline. Estimated energy savings by state-of-the-art light-weighting for each vehicle group have been applied to this differentiated baseline energy consumption (see (IFEU 2004)). Under the assumption that all vehicles in 2000 would have used state-of-the-art light weighting, the global transport energy consumption in 2000 would have been reduced by 2,600 PJ.

The energy consumption of a vehicle group is the most important factor for the total energy savings potential. Therefore, almost 77% of the savings account for the OECD countries. Private passenger cars and light-duty vehicles show the highest total potential for energy savings by light-weighting followed by aircrafts and other road vehicles (**Fig. 3**).

The realisation of energy savings depends on the penetration of light-weight technology in the vehicle fleet which can be encouraged by political and fiscal measures. An almost complete substitution of all vehicles will be accomplished only after 30 to 40 years (e.g. for trains). For certain vehicles (e.g. road vehicles), however, the vehicle turnover rate is much higher, especially in the OECD countries.

5 Conclusions

A weight reduction leads to considerable use phase energy savings for all transport vehicles. However, considerable differences have also been found between the different vehicle groups. These differences can be used to identify priorities for further light-weighting efforts. All energy savings for the use stage are independent of the technical realisation of the weight reduction (e.g. new materials or improved design or logistics). The data can therefore be used in analyses of different light-weighting technologies.

Road vehicles (and especially passenger cars) are estimated to potentially realise the highest overall energy savings as a collective group, but show among the lowest energy savings for a 100 kg weight reduction. Therefore, an analysis of light-weighting options seems to be most important for passenger cars and other road vehicles. The characteristics of new private passenger cars also depend much on the consumer choice, which does not seem to be influenced by fuel consumption. Consumer acceptance and preference for vehicles with low fuel consumption is therefore an important prerequisite to realise further energy savings by light-weighting. If this is taken into account, light-weighting could be one measure towards meeting the target of the ACEA commitment in 2008.

The high use phase energy savings for aircraft, high-speed ferries and also trains, on the other hand, have already been recognised and, therefore, considerable efforts have already been undertaken. This is also due to the fact that, for most commercial vehicles, energy consumption is also a cost factor.

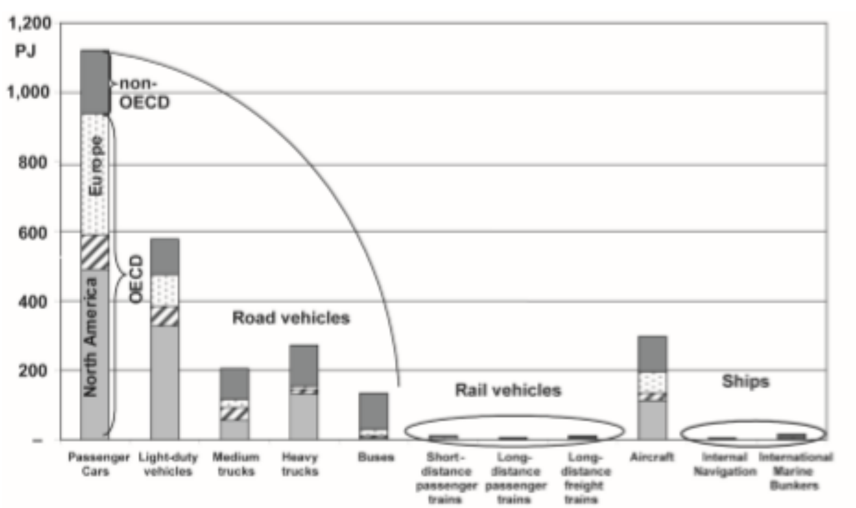

Fig. 3: Potential global annual primary energy savings by light-weighting

On a global scale, it has been shown that the facilitation of light-weighting could make a significant contribution to reduce the global transport energy consumption. The use of light-weighting technology will lead to significant energy consumption benefits in the vehicle fleet after a substantial replacement of the existing fleet with new, weight-reduced vehicles.

6 Recommendations and Perspectives

Light-weighting is one way of reducing transport energy consumption in the use phase. The differences in use phase energy savings for a 100 kg weight reduction between the vehicle groups are considerable and allow for the identification of priorities for future light-weighting efforts.

The contribution to a reduction of the global transport energy consumption, in turn, depends on the further potential for a weight reduction and on the number of vehicles which can be weight reduced. The OECD market of private passenger cars and trucks, for instance, offers a good perspective due to a high contribution to the global transport energy consumption, a considerable potential for weight reduction and a high turnover rate of the vehicle fleet. The benefits will be realised after a substantial replacement of the existing fleet with new, weight-reduced vehicles.

References

Büttner A, Heyn J (1999): Umwelt- und Kostenbilanz im Fahrzeugrohbau: Aluminium, Stahl und Edelstahl. VDI Berichte 1488 137-152. VDI Verlag, Düsseldorf
DB AG (2002): Wissenschaftlicher Grundlagenbericht zum 'UmweltMobil Check' und zum Softwaretool 'Reisen und Umwelt in Deutschland'. IFEU, Heidelberg
Eberle R (2000): Methodik zur ganzheitlichen Bilanzierung im Automobilbau. Dissertation, Technical University, Berlin
Eberle R, Franze A (1998): Modelling the use of passenger cars in LCI. Total Life Cycle Conference Proceedings. Society of Automotive Engineers, Warrendale
Ehinger M, Löffler G, Zeininger H (2000): Nachhaltiges Wirtschaften am Beispiel von Schienenfahrzeugen. Ergebnis Bericht Band 4: Ganzheitlicher Materialeinsatz, Technical University, Dresden
FKA (2002): Lightweight potential of an aluminium intensive vehicle. Final report. Forschungsgesellschaft Kraftfahrwesen, Aachen
FZKA, Achternbosch M, Bräutigam K-R, Kupsch C, Reßler B, Sardemann G (2003): Analyse der Umweltauswirkungen bei der Herstellung, dem Einsatz und der Entsorgung von CFK- bzw. Aluminiumrumpfkomponenten. Institute for Technology Assessment and Systems Analysis. Forschungszentrum, Karlsruhe
Hausberger S, Engler D, Ivanisin M, Rexeis M (2002): Update of the emission functions for heavy duty vehicles in the 'Handbook Emission Factors for Road Traffic'. Institute for Internal Combustion Engines and Thermodynamics. Technical University, Graz
IEA (2003a): Energy statistics of non-OECD countries. International Energy Agency, Paris
IEA (2003b): Energy statistics of OECD countries. International Energy Agency, Paris
IFEU, Helms H, Lambrecht U (2003): Energy savings by light-weighting. Final report for the International Aluminium Institute. Institute for Energy and Environmental Research, Heidelberg
IFEU, Helms H, Lambrecht U (2004): Energy savings by light-weighting – II. Final report for the International Aluminium Institute. Institute for Energy and Environmental Research, Heidelberg
IFEU, Helms H, Lambrecht U (2005): Energy savings by light-weighting for European articulated trucks. Final report for the European Aluminium Association. Institute for Energy and Environmental Research, Heidelberg
INFRAS (1999): Ökoinventar Transport. INFRAS, Zurich
Kelly EK, Davis GA (1998): Comparison of methodologies for calculating use-stage environmental burdens for an automobile. Total Life Cycle Conference Proceedings, Society of Automotive Engineers, Warrendale
KTH/ ETH, Lingg B, Villiger S (2002): Energy and cost assessment of a high speed ferry. KTH Stockholm/ ETH, Zurich
Lufthansa AG (2003): Data via Email Rothmann V. Lufthansa, Frankfurt
MPI (2004): Nestor Baseline Dataset via Email from Leonardi J. Max Planck Institute for Meteorology, Hamburg
Reppe P, Keoleian G, Messick, R, Costic M (1998): Life cycle assessment of a transmission case: Magnesium and aluminium. SAE Technical Paper 980470, Society of Automotive Engineers, Warrendale
Ridge L (1998): EUCAR – Automotive LCA guidelines – Phase 2. Total Life Cycle Conference Proceedings. Society of Automotive Engineers, Warrendale
RWTH, Mandelartz J, Teschers R, Schumacher T (1999): Aluminium Einsatz im Verkehrssektor. RWTH University of Technology, Aachen
Schmidt W-P, Dahlquist E, Finkbeiner M, Krinke S, Lazzari S, Oschmann D, Pichon S, Thiel C (2004): Life-cycle assessment of lightweight and end-of-life scenarios for generic compact class passenger vehicles. Int J LCA 9 (6) 405–416
TREMOD (2005): Transport Emission Model. Software tool developed for the 'Umweltbundesamt' (German Federal Environmental Agency). Institute for Energy and Environmental Research, Heidelberg

Received: September 23rd, 2005
Accepted: July 3rd, 2006
OnlineFirst: July 3rd, 2006

Annex: Suggested average values

Table 2: Suggested average values for end energy savings by light-weighting

Vehicle type	Specific end energy savings per (100 km*100 kg)	Use phase performance (million km)	Use phase end energy savings per 100 kg
Passenger car (Gasoline)	11.3 MJ (0.35 litre)	0.2	23 GJ (700 litre)
Passenger car (Diesel)	10.7 MJ (0.3 litre)	0.2	21 GJ (600 litre)
Articulated truck	2.1 MJ (0.06 litre)	1.2	26 GJ (718 litre)
Subway/ Urban train *	2 MJ (0.56 kWh)	3.0	60 GJ (17 MWh)
Intercity train *	0.4 MJ (0.12 kWh)	8.0	35 GJ (10 MWh)
High-speed train (ICE)*	0.3 MJ (0.08 kWh)	15	44 GJ (12 MWh)
Vehicle type	**Annual end energy savings per 100 kg**	**Use phase (years)**	**Use phase end energy savings per 100 kg**
High-speed ferry **	70 GJ	20	1,400 GJ
Short-distance aircraft **	500 GJ	30	15,000 GJ
Long-distance aircraft **	667 GJ	30	20,000 GJ

* Electricity as energy carrier, end energy data can therefore not directly be compared to fossil fuels

** Ships and aircraft face resistance factors which are entirely different from ground vehicles. Energy savings by weight reduction are therefore not necessarily linear and not expressed as simple coefficients. Values above are derived from specific case studies and converted into comparable reference parameters in order to allow for a comparison with a weight reduction of ground vehicles.